Deep-Sea Research, Vol. 34, No. 4, pp. 565–599, 1987.
Printed in Great Britain.

0198-0149/87 $3.00 + 0.00

Stratification and circulation at the Agulhas Retroflection

ARNOLD L. GORDON,* JOHANN R. E. LUTJEHARMS† and MARTEN L. GRÜNDLINGH†

(*Received* 9 *June* 1986; *in revised form* 6 *October* 1986; *accepted* 14 *October* 1986)

Abstract—The Agulhas Retroflection, as observed in late 1983, consists of the main Retroflection at 21°E with two large warm-core Agulhas rings to its west. The Retroflection position is situated at the eastern-most limit of its range. The ring immediately to the west (Retroflection Eddy) is ellipitical in shape and carries 40×10^6 m^3 s^{-1} relative to the 1500 decibar (db) level; it's core properties are identical to the water enclosed by the Retroflection. These characteristics suggest that the Retroflection Eddy was formed just prior to the field work; thus the west edge of the Retroflection Eddy near 15°E marks the prior position of the main Retroflection, close to the western limit of its range. The second eddy (Cape Town Eddy), centered about 250 km southwest of Cape Town, is circular in form and carries 35×10^6 m^3 s^{-1} relative to 1500 db. It encircles a core of Agulhas water which was highly altered, by the action of the winter atmosphere, from the source Agulhas water. The southwest transport into the main Retroflection through the Agulhas Passage, is 70×10^6 m^3 s^{-1} relative to 1500 db (95×10^6 m^3 s^{-1} relative to the sea floor). Most enters the Retroflection, but 10×10^6 m^3 s^{-1} (relative to 1500 db) continues into the South Atlantic within the region between the two eddies and the African mainland. The magnitude of this flow into the South Atlantic is increased somewhat by the inclusion of South Atlantic Water. The Agulhas Return Current, which receives most of the Agulhas Current transport, flows eastward near 40°S and then executes a "S"-shaped meander over the west half of the Agulhas Plateau to pass eastward within the southern side of the Agulhas Passage.

The Agulhas Current introduces Indian Ocean water masses into the Retroflection region, though this is limited to water less dense than sigma-θ of 27.5, shallower than 1500 or 2000 m. At greater depth, the water flowing within the Retroflection circulation pattern consists primarily of Atlantic and Circumpolar Deep Water. The Indian Ocean Water entering the Retroflection is drawn from diverse sources: the thermocline of the South Indian subtropical gyre, the thermocline water of the western tropical Indian Ocean and within the lower thermocline, remanants of the high salinity–low oxygen water from the Red Sea. Once in the Retroflection region the Indian Ocean Water is altered by the local atmosphere (forming remnant winter mixed layers, marked by relatively high salinity and oxygen) and by low salinity intrusions of South Atlantic Water.

1. INTRODUCTION

THE Subtropical gyre of the South Indian Ocean is composed of two anticyclonic circulation cells. Inspection of the sea surface geopotential topography relative to 3000 db [Plate 388 of WYRTKI, (1971) referred to as W-71] reveals a gyre center near 20° to 25°S at 60°E and another near 35°S at 30°E. In the 500–3000 db map (Plate 389, W-71) the northern cell is no longer evident; it resides only within the upper thermocline where it stretches well into the eastern Indian Ocean. The western boundary current associated with this cell is the East Madagascar Current, which has a poleward transport of 20 Sv (Sv = 10^6 m^3 s^{-1}; WARREN, 1981a) to 41 Sv (LUTJEHARMS *et al.*, 1981). The southern anticyclonic cell persists as depth increases and expands eastward forming a geopotential

* Lamont-Doherty Geological Observatory of Columbia University, Palisades, NY 10964, U.S.A.
† National Research Institute for Oceanology, CSIR, Stellenbosch 7600, South Africa.

crest along 35°S eastward to 80°E and may be related to a crest still further to the east along 45°S which passes to the south of Australia (Plates 388–393, W-71). The weakening and southern displacement of this feature near 90°E occurs at the site of the Ninety-East Degree Ridge. The western boundary current of the southern cell is the Agulhas Current. Geostrophic transport estimates adjacent to Durban are: 44 Sv for the inshore 100 km span, referenced to an average of current profile data (TOOLE and RAYMER, 1985); 62 Sv for the upper 1000 m referenced to direct current observations and up to 75 Sv when these values are extrapolated to the sea floor (GRÜNDLINGH, 1980); and further south near the separation point, a transport of 136 Sv relative to the sea floor (JACOBS and GEORGI, 1977). The wind stress curl across the Indian Ocean at 30°S (HELLERMAN and ROSENSTEIN, 1983) yields 30 Sv transport for the Agulhas Current, based on Sverdrup dynamics, hence the Agulhas, like the Gulf Stream, experiences significant enhancement within a recirculation cell.

In the latitude range 25°–45°S of the western South Indian Ocean there is marked weakening of the thermocline within the 300–600 m interval [Plates 2–21 of the GeoSecs Indian Ocean Atlas, SPENCER *et al.* (1982) referred to as Geosec-Ind]. It is marked by high oxygen concentration spanning a reduced vertical temperature gradient between the 12 and 14°C isotherms, centered in the 26.6–26.7 sigma-θ range (the Geosec-Ind Plates). The existence of the thermostad was noted by COLBORN (1975) who attributed it to thermohaline convection south of the Subtropical Convergence. MCCARTNEY (1977) identified it as the local variety of Subantarctic Mode Water (SAMW). The temperature and salinity distribution suggests that the SAMW is injected mainly near 55°E (W-71, Plates 308–315). The separation of the isopycnals associated with the thermostad deepens the isopycnals of the lower thermocline and thus accounts for the deep reaching characteristic of the southern anticyclonic circulation cell.

The source of Agulhas Current water seems to be primarily within the southern anticyclonic circulation cell, however secondary input from the East Madagascar Current and through the Mozambique Channel is likely. The flow through the Mozambique Channel appears to be quite small: HARRIS (1972) determined a flux of 10 Sv; SAETRE and SILVA (1984) conclude that the Mozambique circulation is dominated by small anticyclonic gyres without appreciable flow through; and FU's (1986) inverse solution for six sections within the Indian Ocean, yields a poleward flux of 6 Sv. While this flow is small compared to the total Agulhas transport, it may be more important to the larger global scale circulation, in that it is associated with the compensating return of water to the Atlantic Ocean required to balance the export of North Atlantic Deep Water (GORDON, 1986). Net poleward transport within the Mozambique Channel is evident in the water properties in that water masses found north of the Mozambique Channel have been traced to positions within the Agulhas system (GRÜNDLINGH, 1985; GORDON, 1986).

The fate of the poleward flow within the East Madagascar Current is not entirely clear. Most of the water appears to be returned to the ocean interior as part of the northern anticyclonic circulation cell, but based on water mass properties some transfer of interior South Indian Ocean Water into the Agulhas system takes place (LUTJEHARMS, 1976). It is likely that much of the water characteristic exchange is achieved by eddies which are cast off an East Madagascar Retroflection adjacent to the southern tip of Madagascar. These eddies then merge with the Agulhas (LUTJEHARMS *et al.*, 1981). However, during the International Indian Ocean Expedition period in the 1960s, the transfer seemed to be more of a steady process (DUNCAN, 1970; GRÜNDLINGH, 1985).

The Agulhas Current turns westward as its path follows the southern terminus of the African continent. Separation from the slope occurs near the Agulhas Bank at 20°–22°E, after which the Agulhas executes an abrupt anticyclonic turn or Retroflection, and the Agulhas Return Current carries the water back into the Indian Ocean (BANG, 1970; HARRIS and VAN FOREEST, 1978). The Agulhas Return Current responds to the topographic features of the Agulhas Plateau and Mozambique Ridge with a cyclonic loop northward, which may initiate planetary waves in the downstream path of the Return Current (DARBYSHIRE, 1972; LUTJEHARMS and VAN BALLEGOOYEN, 1984; HARRIS *et al.*, 1978). The Agulhas, it's Retroflection and the Agulhas Return Current enclose a pool of relatively warm water, which on exposure to the colder atmosphere supports large average annual heat flux into the atmosphere, in excess of 100 W m^{-2} (BUNKER, 1980). Not all of the Agulhas transport participates in the Agulhas Retroflection; some transport into the South Atlantic occurs. This is seen in the 19th century surface current charts of the region (PEARCE, 1980) and in hydrographic studies (DIETRICH, 1935; HARRIS and VAN FOREEST, 1978; GORDON, 1985). The amount of leakage into the Atlantic is small relative to the Agulhas Current, amounting to 5–14 Sv, about 10–20% of the full transport. This interocean transfer would also be part of the global scale circulation pattern referred to above (GORDON, 1986). The dynamics of the Agulhas Retroflection region is examined by DE RUIJTER (1982) and OU and DE RUIJTER (1986).

The Agulhas Retroflection is associated with a very active mesoscale field. The sea level change measured during the SEASAT period in 1978 indicates the highest

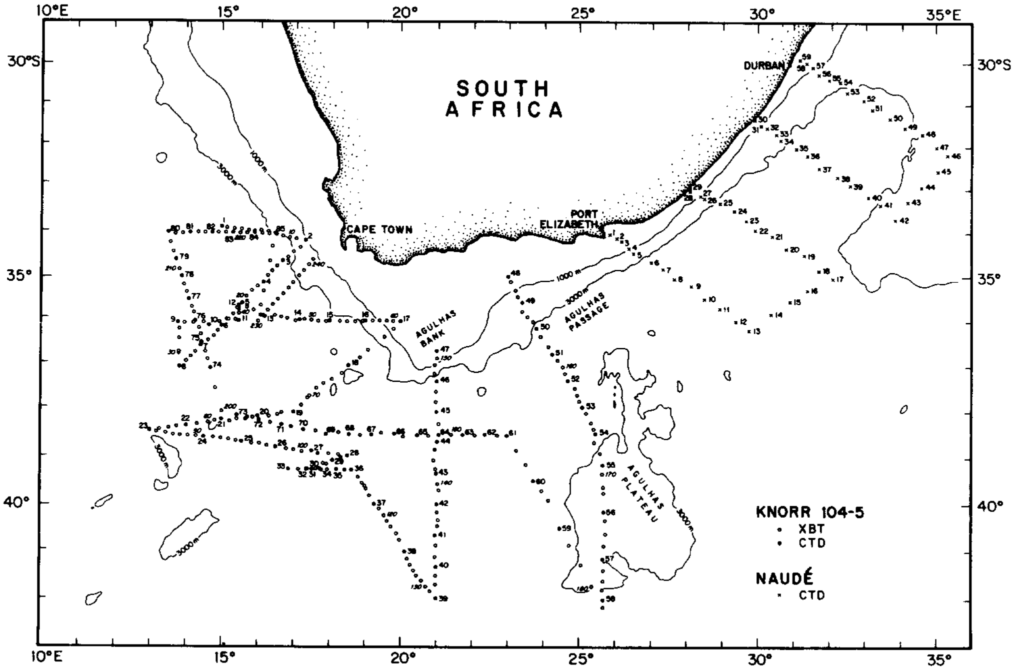

Fig. 1. Distribution of CTD hydrographic stations and XBT observations obtained from the R.V. *Knorr* [November–December 1983; HUBER *et al.* (1986) reports the CTD station data; HAINES *et al.* (1984) reports the XBT data] and CTD hydrographic stations obtained from R.V. *Meiring Naude* (October 1983; GRÜNDLINGH, 1986). The 3000 m isobath is taken from the GEBCO chart.

variability found in the southern hemisphere occurs off South Africa, as high as 40 cm (CHENEY *et al.*, 1983; COLTON and CHASE, 1983). Variability is most intense between 11° and 16°E (Fig. 7 of CHENEY *et al.*, 1983; also see Fig. 10 of COLTON and CHASE, 1983). Variability is also revealed in the surface temperature patterns observed from satellite (HARRIS *et al.*, 1978; LUTJEHARMS, 1981a), from satellite-tracked drifters (GRÜNDLINGH, 1977, 1978; PATTERSON, 1985) and from hydrographic data (DUNCAN, 1968; LUTJEHARMS, 1981a). The variability is dominated by shear edge eddies along the inshore side of the Agulhas and by changes in the position of the Retroflection associated with generation of warm-core rings (LUTJEHARMS, 1981b; OLSON and EVANS, 1986).

In November–December 1983 the R.V. *Knorr* obtained an array of CTD/Rossette hydrographic stations and expendable bathythermographs (XBT) within the Agulhas Retroflection region (Fig. 1; HAINES *et al.*, 1984; CAMP *et al.*, 1986). The objective of the program was to resolve the thermohaline, oxygen and nutrient structure of the waters composing the Retroflection and to set out a series of satellite-tracked drifters within appropriate features. During the preceding month the R.V. *Meiring Naude* obtained a CTD grid of stations to the northeast of the Agulhas Passage (Fig. 1; GRÜNDLINGH, 1986) to define the oceanic characteristics upstream of the Retroflection. These data sets are used here for a detailed study of the baroclinic mass balance of the Agulhas Retroflection and of water mass composition and origin within the region. The only other survey that approaches these data sets in synopticity was obtained in March 1969 and discussed by HARRIS and VAN FOREEST (1978). The drifter data from the 1983 program are discussed by OLSON and EVANS (1986).

2. BAROCLINIC STRUCTURE

Dynamic topography

The geopotential anomaly of the sea surface relative to 1500 db (0/1500; Fig. 2) reveals a geostrophic circulation pattern remarkably similar to that found in March 1969 (HARRIS

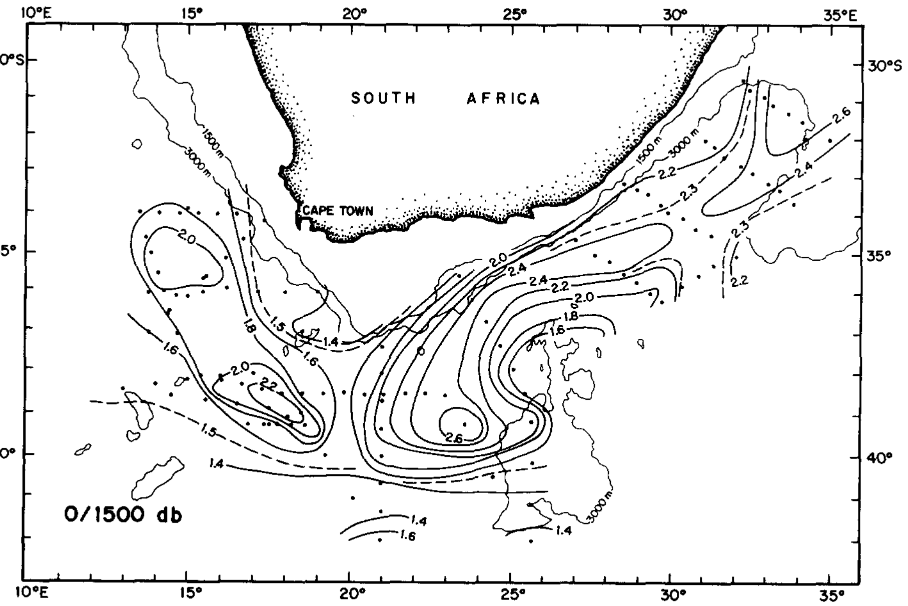

Fig. 2. Dynamic height anomaly of the sea surface relative to the 1500 decibar (db) surface. Values are given in dynamic meters.

and VAN FOREEST, 1978). The axis of the Agulhas Current east of the Agulhas Passage is strongly pressed up against the continental slope, and is not well defined by the *Meiring Naude* 0/1500 db pattern. However, the ship drift data indicate that the axis is over the upper slope, landward of the inshore station (GRÜNDLINGH, 1986). GRÜNDLINGH (1983) finds that the intersection of the 15°C isotherm with the 200 m depth horizon defines the axis of flow (a situation similar to that of the Gulf Stream). This position, for the most part, is found within a few tens of kilometers from the shelf break, and over the 500–2400 m isobath of the continental slope from Durban to Port Elizabeth (see Table 1 from GRÜNDLINGH, 1983). The seaward meander marked by the Sta. 30 to 42 section (Fig. 2), is a fairly common event (GRÜNDLINGH, 1978, 1986).

The Agulhas Current separates from the continental slope near 22°E, though the 0/1500 pattern suggests more gradual seaward spreading of the current axis as the current continues westward from the Agulhas Passage. The southward flow along 20°–22°E marks the west wall of the Agulhas Retroflection (called the main Retroflection in this paper). It is centered at Sta. 60 with a dynamic height anomaly of 2.61 dyn m relative to 1500 db. The lowest dynamic height found south of the Agulhas Return Current of 1.28 at Sta. 38, indicates that the regional sea level relief (relative to the 1500 db) is slightly above 1.3 m.

The west wall of the main Retroflection occurs at the eastern limit of its range, as defined by satellite i.r. data (HARRIS *et al.*, 1978); the western limit falls near 14°E, a condition found by drifter 1210 in mid-December 1976 (GRÜNDLINGH, 1978). It is likely that the anticyclonic eddy immediately to the west (called the Retroflection Eddy in this paper) of the main Retroflection was only recently spawned, indicating a Retroflection position closer to 15°E, prior to the *Knorr* cruise. The highly elliptical form of the Retroflection Eddy (semi-major and semi-minor axis of 125 and 50 km, respectively) may be indicative of its recent generation (OLSON and EVANS, 1986); furthermore the similarity of the core water properties of the Retroflection Eddy with those within the main Retroflection (discussed below) support that contention. The i.r. images from the METEOSAT II show continued northward growth of a cold water feature separating the Retroflection Eddy from the main Retroflection (LUTJEHARMS and GORDON, in preparation). The Retroflection Eddy moves towards the west-northwest at a rate of 8.5 cm s^{-1} during the period of tracking by drifters (OLSON and EVANS, 1986).

To the northwest of the Retroflection Eddy is another anticyclonic feature (called the Cape Town Eddy in this paper). Its more circular form, with a radius of about 100 km. and the highly altered water properties within its core relative to the main Retroflection (discussed below) indicate it is older than the Retroflection Eddy. It is possible the Cape Town Eddy eventually drifted further into, and ultimately dissipated, within the South Atlantic; a previous "Cape Town Eddy" may be the origin of a large mesoscale feature observed well into the South Atlantic by MCCARTNEY, RAYMER and COLLINS (in preparation). The Cape Town Eddy translation during drifter tracking period was towards the west-northwest at 4.8 cm s^{-1} (OLSON and EVANS, 1986). OLSON and EVANS (1986) show that the two eddies observed during the program are 4 times more energetic relative to other western boundary generated eddies and rings. This is particularly significant in that the Agulhas eddies impinge on a relatively quiescent eastern boundary regime.

Between the two eddies and the African continental margin there is evidence of flow into the South Atlantic (called the Cape Town Jet by OLSON and EVANS, 1986). This is shown by: the geostrophic circulation (GORDON, 1985; and discussed below); the trajectories of satellite-tracked drifters set out from the *Knorr* (OLSON and EVANS, 1986); and by the surface temperature pattern, which shows a warm water branch stretching northward to the landward of the eddies (GORDON, 1985). The branching feature is more obvious in the higher resolution map of the 10°C isotherm depth (which is a useful proxy for dynamic height, since the dynamic topography bears a nearly linear relationship with thermocline depth) presented by GORDON (1985). The penetration of warm surface water into the South Atlantic close to the continent is also noted by HARRIS *et al.* (1978). BANG (1973) noted the presence of an intrusion of "pure" Agulhas Current water west of Cape Town. This warm water feature forms a sharp front over the shelf break as it contacts the colder upwelled water over the shelf. BANG and ANDREWS (1974) showed that this shelf edge front is associated with intense northward flow, amounting to a total of 7 Sv. They called this feature the Good Hope Jet. They further noted ". . .vestiges of Agulhas Bank or Agulhas Current water are almost always found outside the Cape upwelling cell in summer," and that seaward of this water is general anticyclonic circulation. The Cape Town Jet is over deeper ocean than the Good Hope Jet, but some relationship is probable.

The Agulhas Return Current undergoes an "S"-shaped meander over the Agulhas Plateau, passing to the east of 26°E within the Agulhas Passage. This pattern appears so frequently that it has now entered into the schematic representations of the Agulhas Retroflection (LUTJEHARMS, 1981a). Perhaps it should be considered a quasi-stationary feature of the Agulhas Retroflection. The deflection of the Agulhas Return Current over the 1500–2000 m deep central region of the Agulhas Plateau indicates that the current extends to at least that depth. However, the current does cross the 3000 m isobath of the Plateau's western flank, suggesting that it may not reach that depth or at least is weak at 3000 m. The cyclonic turn around Stas 53 and 54 may spawn cold-core eddies into the main Retroflection; such a feature was observed in the Retroflection in a January 1985 survey from the R.V. *Thomas Washington* (BENNETT *et al.*, 1985).

The R.V. *Meiring Naude* data show that the Agulhas Return Current turns to the south near 35°S and 30°E, with some partial return to the north near 32°E. The continuity of the dynamic topographic crest of the Agulhas Retroflection is interrupted across the *Meiring Naude* Sta. 17 to 29 section, giving the appearance that the Agulhas Current is composed of a series of anticyclonic features (GRÜNDLINGH, 1986).

The 1.4 dyn m isobath along 40°–41°S is associated with Atlantic Water flowing eastward. However, to the south, at Sta. 39 and at Sta. 58, there is a return to higher dynamic elevations, with water mass characteristics similar to Indian Ocean Water. This point is returned to below, but it appears that anticyclonic eddies which form in the Retroflection region pass back into the Indian Ocean to the south of the main Retroflection and may be re-absorbed by the main Retroflection.

Geostrophic velocity and transport

Geostrophic velocity and volume transport relative to 1500 db are shown for three *Knorr* sections within the Agulhas Retroflection region (Figs 3a–c). (The corresponding thermohaline, oxygen and silicate sections, as well as other sections constructed from the *Knorr* and *Meiring Naude* data are available upon request from the authors of this paper.) The 1500 db reference is used for a variety of reasons: (1) The Agulhas Current axis, when following the continental margin, is mostly confined landward of the 2000 m isobath [PEARCE (1977) found that peak velocity occurs on an average at 52 km offshore of

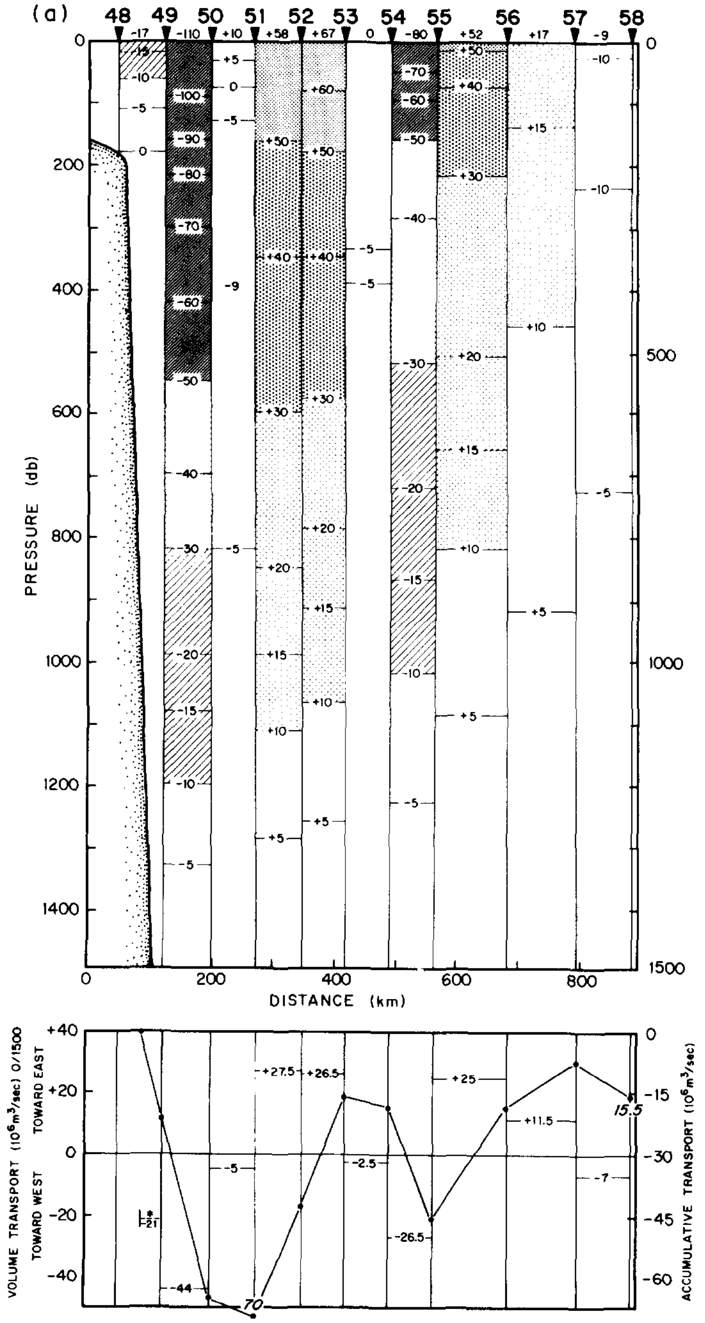
(a)
48 49 50 51 52 53 54 55 56 57 58
PRESSURE (db)
DISTANCE (km)
VOLUME TRANSPORT (10^6m^3/sec) 0/1500
TOWARD EAST
TOWARD WEST
ACCUMULATIVE TRANSPORT (10^6m^3/sec)

Fig. 3a.

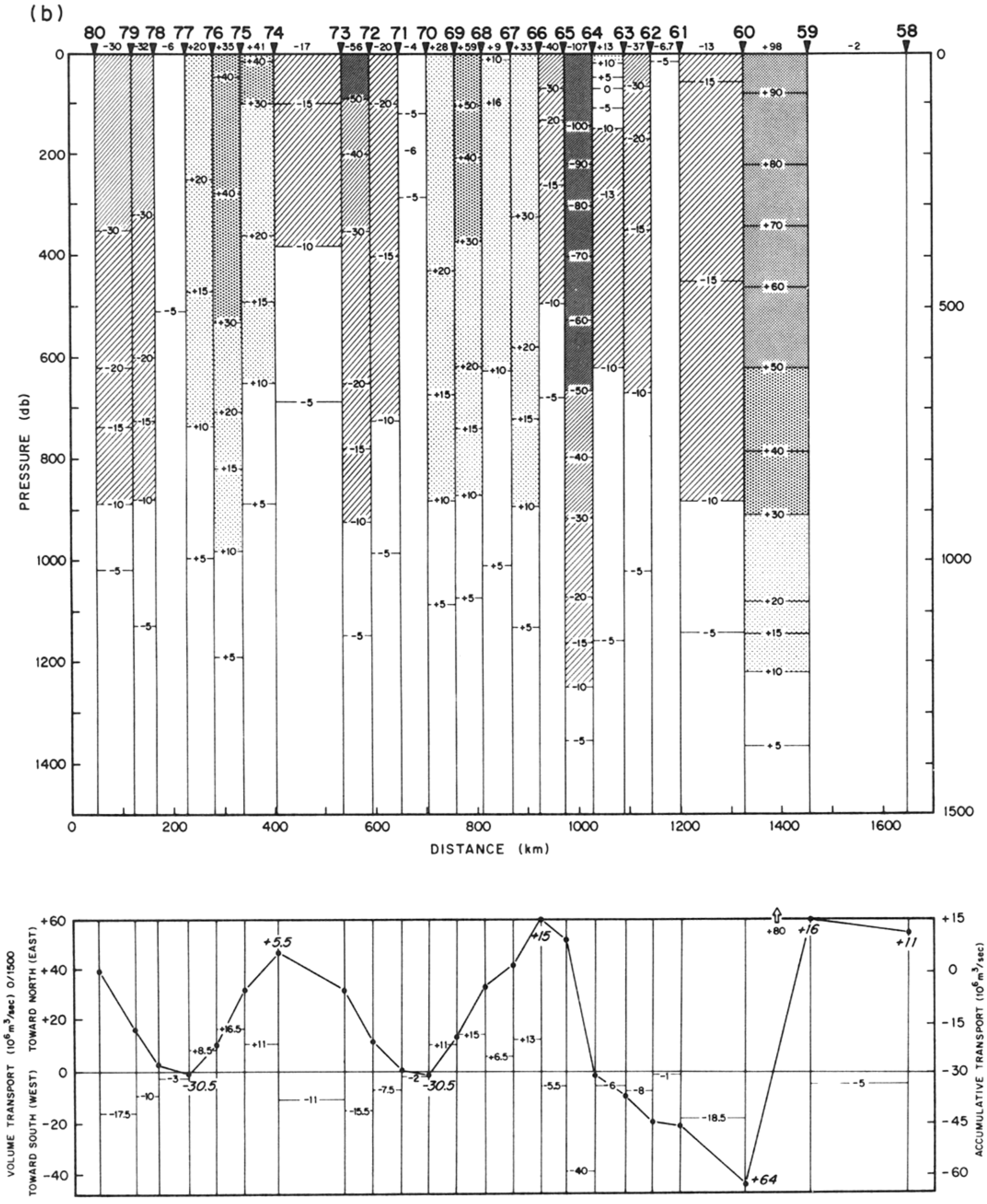
(b)
80 79 78 77 76 75 74 73 72 71 70 69 68 67 66 65 64 63 62 61 60 59 58
PRESSURE (db)
DISTANCE (km)
VOLUME TRANSPORT (10⁶m³/sec) 0/1500
TOWARD NORTH (EAST)
TOWARD SOUTH (WEST)
ACCUMULATIVE TRANSPORT (10⁶m³/sec)

Fig. 3b.

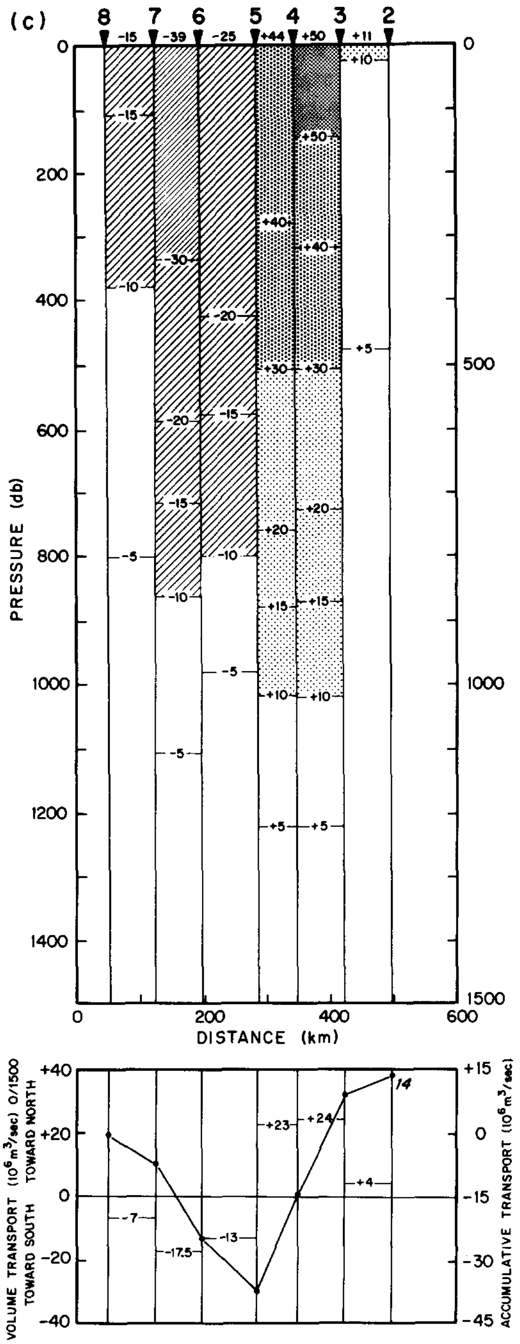

Fig. 3. (a) Upper panel: geostrophic velocity perpendicular to the section of Stas 48–58, relative to 1500 db surface. Positive values are directed to the east, negative to the west. Lower panel: volume transport between stations pairs (left scale) in Sv; and accumulative volume transport (right scale, and the solid line) from the northern-most station pair. The starred value for the transport between Stas 48 and 49 is an extrapolation of the transport function of station pair 49–50 a distance of 20 km to the north so as to include the segment of the Agulhas north of Sta. 49. (b) Same as (a), for Stas 58–80. Positive values are for flow directed to the north, negative for flow to the south. (c) Same as (a), but for Stas 2–8. Positive values are for flow directed to the north, negative for flow to the south.

Durban (GRÜNDLINGH, 1983; TOOLE and RAYMER, 1985)] thus a reference layer of 2000 db would miss a significant component of the current; (2) to obtain the extensive grid of stations from *Knorr* in the time allotted not all stations extend to the sea floor (31% reaches to the sea floor deeper than 1500 m); (3) inspection of the baroclinic volume transport for the bottom reaching stations finds that in the interval 1500–3000 db the transport amounts to only 15–25% of that between the surface and 1500 db. This result is similar to that reported by DUNCAN (1970): that 83% of the Agulhas Current off the southeast coast of Africa resides within the upper 1000 m.

Section 48–58 (*Fig.* 3*a*). This section, the eastern-most of the *Knorr* grid, crosses the Agulhas Current input to the Agulhas Retroflection region and the "S"-shaped meander traced by the Agulhas Return Current. The thermal section constructed of the combined CTD and XBT data (Fig. 4) reveals a region of strongly sloped isotherms from the positions of XBT 156 and CTD 50 landward to XBT 152 and 153, a distance of 90 km. This marks the width of the westward-flowing Agulhas Current, a width similar to that found upstream (GRÜNDLINGH, 1980). The warmest surface water of the section marking the Agulhas warm core is located at the seaward edge of the zone. The "S"-shaped meander associated with the Agulhas Plateau is clearly revealed in the thermal structure: XBT 170 defining the center of the anticyclonic turn and XBT 165–166 defining the cyclonic turn, which directs the flow through the Agulhas Passage. Between XBT 172 and CTD 56 is a strong thermal front. This feature falls just to the south of the Agulhas Return Current and may mark the combination of the Agulhas Front and the Subtropical Convergence (LUTJEHARMS and VALENTINE, 1984).

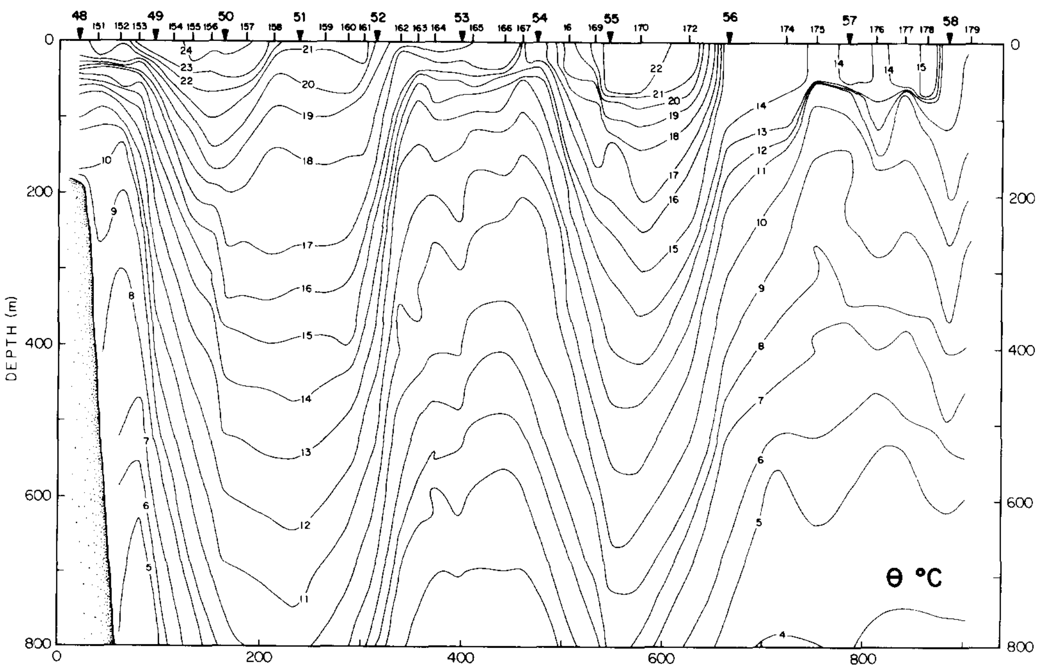

Fig. 4. Potential temperature section constructed from CTD and XBT data from CTD Sta. 48 to XBT 179.

The slight increase in surface temperature and the tilt down towards the south of the isotherms south of CTD 57 marks the anticyclonic feature observed on the 0/1500 db map (Fig. 2), which, based on water properties, appears to be an eastward drifting "old" warm-core ring of the Agulhas.

The geostrophic velocity relative to 1500 db (Fig. 3a) shows an average surface flow of 110 cm s^{-1} between Stas 49 and 50 which span the Agulhas inflow. This is similar to drifter velocities in the same positions, which range from 90 to 119 cm (Figs 2a and 4 from GRÜNDLINGH, 1978). PEARCE (1977) determined a peak surface flow adjacent to Durban of 136 cm s^{-1}. The surface flow associated with the "S"-shaped meander ranges from 52 to 80 cm s^{-1} (perpendicular to the section). At station pair 50–51 the surface flow is directed to the east, but below 100 m the flow reverses, producing a maximum to the west of 9 cm s^{-1} at 400 m. This condition is seen in the direct current observations reported by GRÜNDLINGH (1980), where reverse shear is observed from the surface to the maximum flow near 100–200 m, adjacent to Durban. The Agulhas Current is marked by an offshore migration of the axes of flow as depth increases, as is the case with the Gulf Stream (RICHARDSON and KNAUSS, 1971).

The volume transport (lower panel of Fig. 3a) yields 49 Sv across the station pairs 49–50 and 50–51. However, the thermal section (Fig. 4) indicates that the Agulhas extends another 20 km landward of Sta. 49. Extrapolation of the transport function for the 49–50 station pair across that distance yields an additional 21 Sv, bringing the total Agulhas Current transport into the Retroflection region to 70 Sv. This is about the average value given by GRÜNDLINGH (1980) for the full depth Agulhas transport off Durban and Port Edward further upstream.

The 6 Sv growth per 100 km distance referred to by GRÜNDLINGH (1980) is based on the difference between Durban (full depth) transport and the 136 Sv estimate for the transport adjacent to the Agulhas Bank relative to the sea floor, given by JACOBS and GEORGI (1977). The Agulhas full depth transport across the eastern *Knorr* section (Stas 48–51) would increase to 74 Sv, referenced to the sea floor. Including the 21 Sv adjustment made for the Agulhas flow landward of Sta. 48 (as discussed above), the full depth transport is 95 Sv. With this value, the growth rate from Durban to the Agulhas Passage is 2.7 Sv per 100 km. Using the *Knorr* results with the Jacobs and Georgi value (note their value does not include a correction for the "missing" area adjacent to the continental slope), the growth rate from the Agulhas Passage to Agulhas Bank amounts to 13 Sv per 100 km. Thus it appears that the 6 Sv per 100 km growth rate does not apply to the 1983 situation or at the very least, the growth rate from Durban to Agulhas Passage is much less than that within the Retroflection west of Agulhas Passage. A larger growth rate west of Agulhas Passage would indicate significant re-circulation within the Retroflection. This may be particularly the case for the deep water (discussed below) in that there does not seem to be very much deep water from the interior of the Indian Ocean within the Retroflection region.

The transport relative to 1500 db, within the Agulhas Return Current passing to the east through the Agulhas Passage is 54 Sv (station pairs 51–52 and 52–53) producing a miss-match of 16 Sv between inflow and outflow (the miss-match across the entire section is effectively the same). The imbalance could be accounted for by westward growth of the Retroflection region of approximately 3.0 cm s^{-1} or by a loss of water to the Atlantic Ocean, which is then returned at greater depth and/or to the south of the Agulhas Return Current (GORDON, 1985).

Section Stas 58–80 (*Fig.* 3*b*). This section traverses more-or-less zonally the main Retroflection, the Retroflection Eddy and the western edge of the Cape Town Eddy. The combined XBT and CTD thermal section across the central part of the section (Fig. 5), shows the strongly sloping isotherms and warm surface water marking the poleward flow of the Agulhas Current around the main Retroflection between CTD 64 and 66. A warm surface water feature of <100 m thickness, slips further to the west of the thermocline expression, reaching to CTD 67. This suggests caution in interpreting surface water patterns in terms of deeper baroclinic structure. Colder subsurface water between CTD 66 and XBT 194, associated with the trough in sea level (Fig. 2), separates the main Retroflection from the Retroflection Eddy. The Retroflection Eddy is observed between XBT 194 and CTD 73. Reduced thermal gradients are found near the 18°C isotherm in the main Retroflection and Retroflection Eddy and near the 16°C isotherm of the Cape Town Eddy (Fig. 6). At 600 m at Sta. 60 is an additional region of reduced gradient near the 13°C isotherm (seen in the profiles shown in Fig. 14, discussed below). The layers of reduced vertical gradients are referred to as pycnostads. They are associated with positive salinity anomalies and high oxygen relative to the Agulhas inflow characteristics and are believed to be products of local thermohaline modification. The point is discussed in Section 4.

The relative geostrophic velocity within the poleward-flowing Agulhas forming the west wall of the main Retroflection is 107 cm s^{-1} (between station pair 64–65). Peak velocities associated with the Retroflection Eddy are 56–59 cm s^{-1}. The drifter data

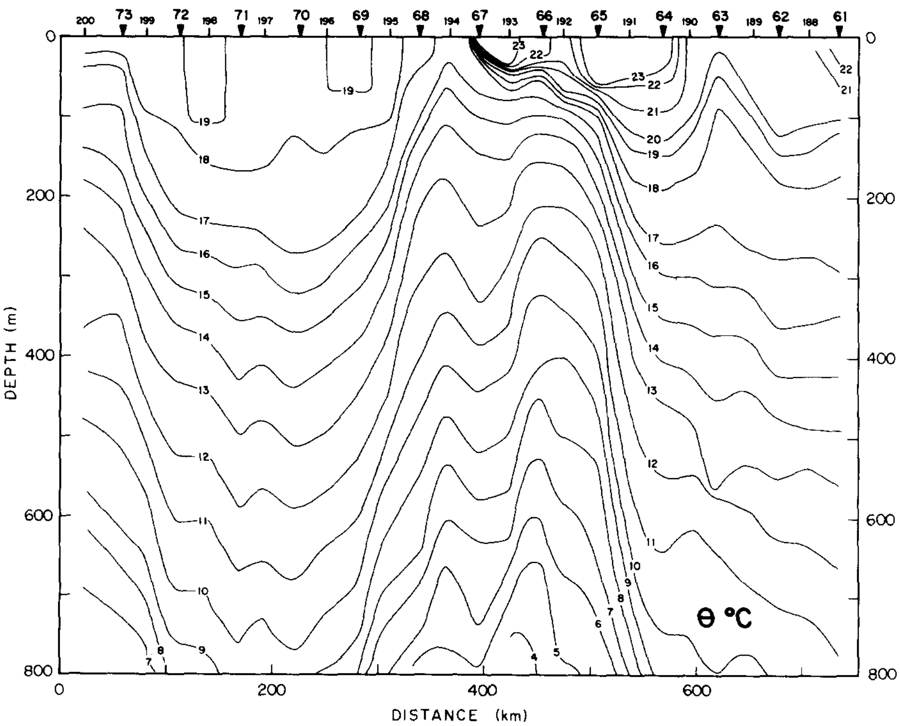

Fig. 5. Same as Fig. 4 for the section from CTD 61 to XBT 200.

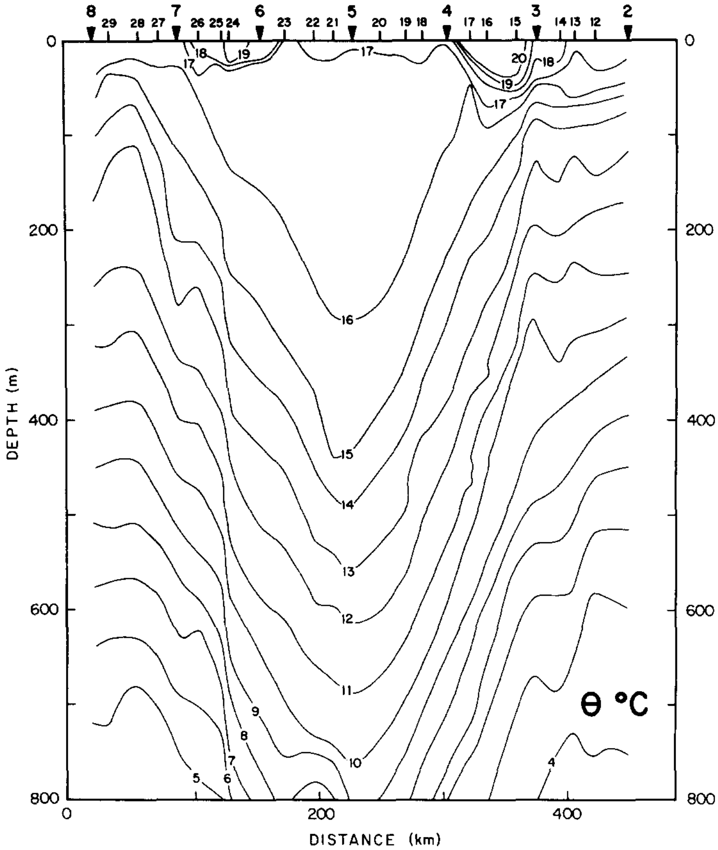

Fig. 6. Same as Fig. 4 for the section from CTD Sta. 2 to CTD Sta. 8.

(Fig. 5 of Olson and Evans, 1986) indicate a range in speeds of 60–80 cm s^{-1}. The Agulhas Return Current between Stas 59 and 60 shows surface flow of 98 cm s^{-1}.

Section Stas 2–8 (*Fig.* 3*c*). Stations 2–8 cross the Cape Town Eddy (also see Fig. 6). The northward-flowing edge lies between CTD 3 and 5, and the southward flow is defined by CTD 5 to XBT 28. Warm surface water associated with the Agulhas axis, though cooler than observed at the inflow to the Retroflection region, is found between station pairs 3–4 and 6–7. This feature influences the density field, inducing a cyclonic "lid" over the core of the otherwise anticyclonic eddy. This situation is also observed within the warm-core eddies of the Gulf Stream system (e.g. Joyce *et al.*, 1983). The thick isothermal core of 16°C water is believed to be a modified form of the 18° thermostad within the main Retroflection, this point is discussed in Section 4.

The surface geostropic velocities relative to 1500 db are near 50 cm s^{-1} on the northward-flowing edge, but only near 40 cm s^{-1} along the western edge. The intensification of the northward flow to the east of the Cape Town Eddy center is clearly seen in the drifter data. Olson and Evans (1986) call this flow the Cape Town Jet; their Fig. 5 shows drifter speeds ranging from 25 to 75 cm s^{-1} around the eddy center, with the higher speeds associated with the trajectories east of the eddy center. The net volume transport across the Cape Town Eddy relative to 1500 db is 14 Sv (Gordon, 1985), which may account for the imbalance across the Sta. 48–58 section, suggesting a net flow into the South Atlantic.

Geostrophic transport pattern

The volume transport for the upper 1500 db of the water column relative to the 1500 db level, is determined from a broad selection of station pairs in order to establish the overall transport pattern of the Agulhas Retroflection during the November–December 1983 period. The schematic representation of this pattern (Fig. 7) provides transport values to the nearest 5 Sv for the upper 1500 db (again relative to the 1500 db level); the pattern is guided by the 0/1500 dynamic topography (Fig. 2) and specific transport values calculated from station pairs. The circled transport values associated with the dashed arrow inshore of the *Meiring Naude* station grid are inferred to maintain continuity with the 70 Sv transport value for the Agulhas Current crossing the easternmost *Knorr* section.

The 70 Sv Agulhas Current input to the Retroflection region splits: 60 Sv enter into the main Retroflection and Agulhas Return Current while 10 Sv continue to flow west to feed two thirds of the imbalance associated with the Cape Town Eddy. The other 5 Sv are derived from colder South Atlantic water entering the system from the south, around the Retroflection Eddy. Thus the Cape Town Eddy imbalance is not totally derived from the Agulhas Current, but includes South Atlantic Water. The basic transports associated with the Retroflection and Cape Town Eddies are 40 and 35 Sv, respectively. The water mass blending is discussed in the water mass section below.

The transports associated with the anticyclonic eddies south of the Agulhas Return

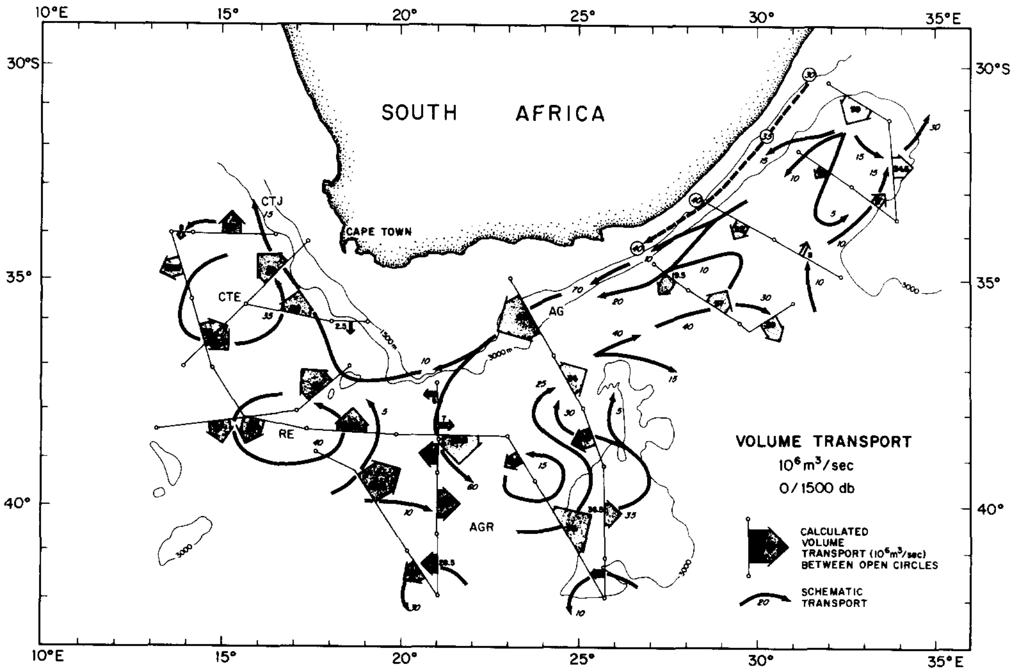

Fig. 7. Volume transport for the upper 1500 db relative to the 1500 db surface (see text).

Current are 30 Sv for the eddy at 21°E and 10 Sv for the one at 26°E. However these features are probably not fully resolved with the data set. Within the main Retroflection there is a small enclosed anticyclonic circulation, around Sta. 60, amounting to 15 Sv. The "S"-shaped meander executed by the Agulhas Return Current over the Agulhas Plateau involves about 55 Sv, with the remaining 5 Sv not resolved by the eastern-most *Knorr* section.

Within the southwestern section of the R.V. *Meiring Naude* station grid the Agulhas Return Current turns poleward, though 10 Sv curl back into the Agulhas Current. The possibility cannot be ruled out that the cyclonic feature centered at *Meiring Naude* Sta. 12, is part of an eddy spawned from the equatorward loop over the Agulhas Plateau (GRÜNDLINGH, 1986). The 80 Sv of Agulhas transport across the northern-most *Meiring Naude* section split: 60 Sv continue along the continental margin (which on joining with the 10 Sv from the Agulhas Return Current, compose the 70 Sv input to the Retroflection region); and 20 Sv turn back to north, which on joining with another 10 Sv from the Agulhas Return Current, yield a total of 30 Sv directed towards the northeast.

3. WATER MASSES OF THE AGULHAS RETROFLECTION

Water masses of the western Indian Ocean

To address the water mass composition and origins of the Agulhas Retroflection region it is necessary to first discuss the water masses of the western Indian Ocean.

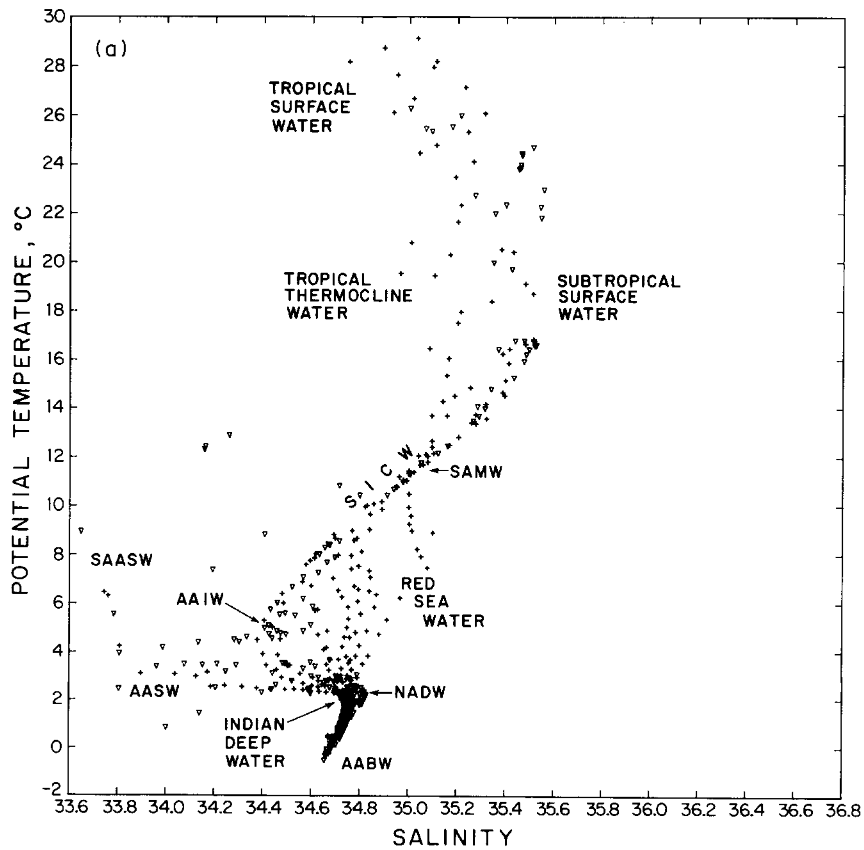

Fig. 8a.

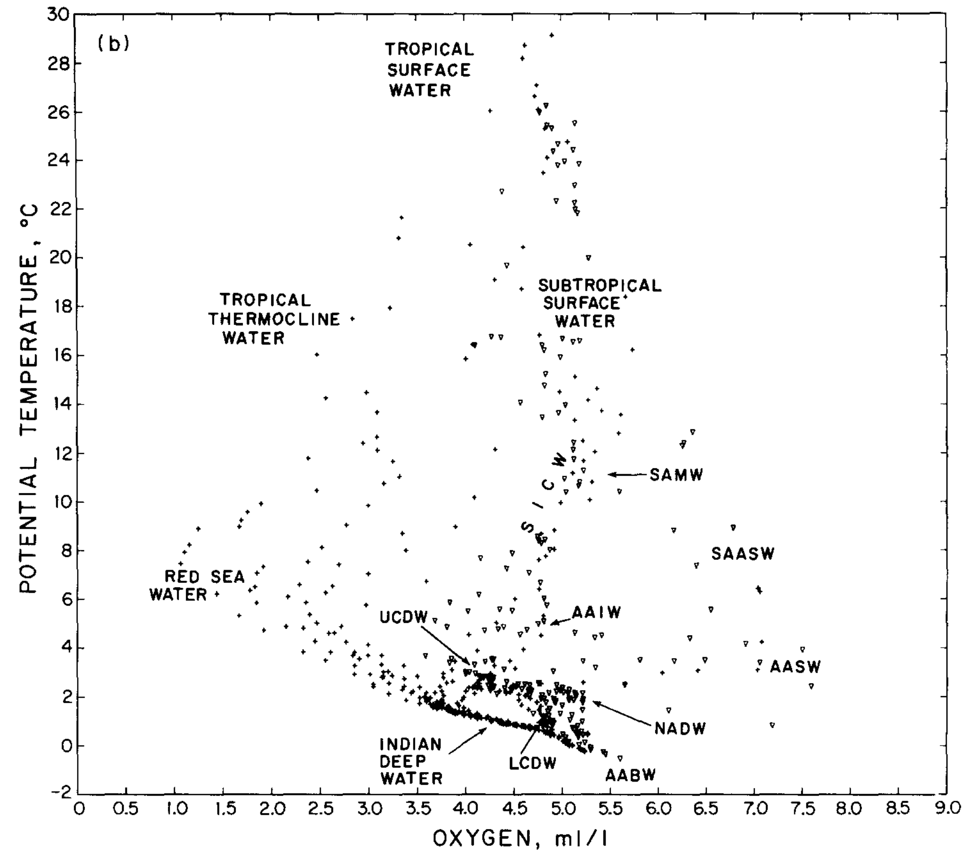

Fig. 8. (a) Potential temperature vs salinity distribution for the western Indian Ocean using Geosecs Stas 420–429 (SPENCER et al., 1982) and select stations from CONRAD 17 (JACOBS and GEORGI, 1977). SICW, South Indian Central Water; SAMW, Subantarctic Mode Water; NADW, North Atlantic Deep Water; AABW, Antarctic Bottom Water; AASW, Antarctic Surface Water; AAIW, Antarctic Intermediate Water; SAASW, Subantarctic Surface Water. (b) Potential temperature vs oxygen based on the same data used in (a). Same water mass abbreviations; LCDW, Lower Circumpolar Deep Water; UCDW, Upper Circumpolar Deep Water.

Salinity and oxygen data plotted against potential temperature for a selection of Geosecs and CONRAD 17 data for the western Indian Ocean (Figs 8a and b, respectively) display the large range of water properties from which the Agulhas Current can draw. Reference can be made to the W-71 and Geosecs-Ind atlases and to WYRTKI (1973), IVANENKOV and GUBIN (1960), PEARCE (1977), JACOBS and GEORGI (1977), and WARREN (1981a) for a discussion of various water masses of the western Indian Ocean.

The surface water in the tropical zone (Tropical Surface Water in Fig. 8) is relatively fresh as excess precipitation and inflow from the Pacific through the Indonesian Seas depress salinities. Further south, surface salinity is higher as the excess evaporation subtropical zone 25°–35°S is encountered. The subtropical water sinks, producing subsurface salinity maximum at temperatures near 18°C (Subtropical Surface Water in Fig. 8) throughout the South Indian Ocean. In the tropical region, water of similar temperature is significantly lower in salinity and in oxygen (Tropical Thermocline Water in Fig. 8). A shallow oxygen minimum south of 10°S (Geosecs-Ind) is a consequence of reversal in oxygen gradient associated with the deeper oxygen maximum of the SAMW (Colborn, 1975; McCartney, 1977) thermostad, introduced along the southern edge of the subtropical region. Warren (1981b) suggests that the shallow oxygen minimum may not represent southward flow but rather the effects of oxygen consumption (that decreases rapidly with depth) on slowly moving northward flow. The core layer maps of the shallow oxygen feature provided in W-71 (Plates 300–307) show the low oxygen extends to the south within the western margins of the Indian Ocean. It is likely that while northward drift may be the case within the interior, southward flow occurs along the western boundary as part of the gyre system.

The South Indian Central Water (SICW) or thermocline water spans the interval from the more saline surface water to the salinity minimum of the Antarctic Intermediate Water (AAIW). The SAMW feature falls within the SICW curve near the 12°C isotherm. North of 15°S the salinity minimum gives way to more isohaline stratification, and in these "more northern latitudes the appropriate density interval is occupied by very saline water from the Arabian Sea (deriving its characteristics mainly from the Red Sea outflow . . ." (Warren, 1981a). The high salinity and low oxygen of the Red Sea water mass are clearly revealed in Fig. 8.

The deep water within the western Indian Ocean is dominated by the North Atlantic Deep Water (NADW), marking a local salinity maximum and by the slightly less saline Indian Deep Water. The Indian Deep Water is associated with much lower oxygen than is the NADW, forming two distinct modes in potential temperature–oxygen space. Warren (1981a) points out the similarity of this feature with a deep oxygen minimum in the South Pacific, both of which he suggests flow to the south from their generation region in low and northern latitudes.

In the Southern Ocean sector the NADW lies between two layers of Circumpolar Deep Water (CDW, subdivided into Upper and Lower CDW). The Deep Indian Water regime in θ/O_2 space shows no effect of CDW. The CDW–NADW layers and the Indian Deep Water regime appear to be two distinct types of deep stratification. The bottom water is marked by cold, high oxygen Antarctic Bottom Water (AABW). At the surface in the Southern Ocean regime are the low salinity Antarctic and Subantarctic Surface Water masses (AASW and SAASW, respectively).

Water masses—R.V. Meiring Naude *data set*

The potential temperature–salinity relation of the data obtained by the *Meiring Naude* (Fig. 9) reveals a variety of western Indian Ocean water masses. The dominant signal, as expected from the principal source of the Agulhas Current, is the Subtropical Surface Water, SICW, and AAIW (the stations were taken only to 2000 m and hence do not reach the deep water masses). However, the inshore stations tend to have much lower salinities in the temperature interval 16–20°C. Further offshore, this temperature interval is dominated by the more saline subtropical salinity maximum derived from Subtropical Surface Water. The sections between Richards Bay and Port Edward, shown by Pearce (1977) also reveal that the subsurface salinity maximum occurs towards the offshore side of the Agulhas. The inshore, relatively low salinity water in the 16–20°C range can be traced to the Mozambique Channel (Gordon, 1986) and, by the associated shallow oxygen minimum core layer maps (W-71, Plates 300–308), to the Tropical Thermocline Water of the western Indian Ocean.

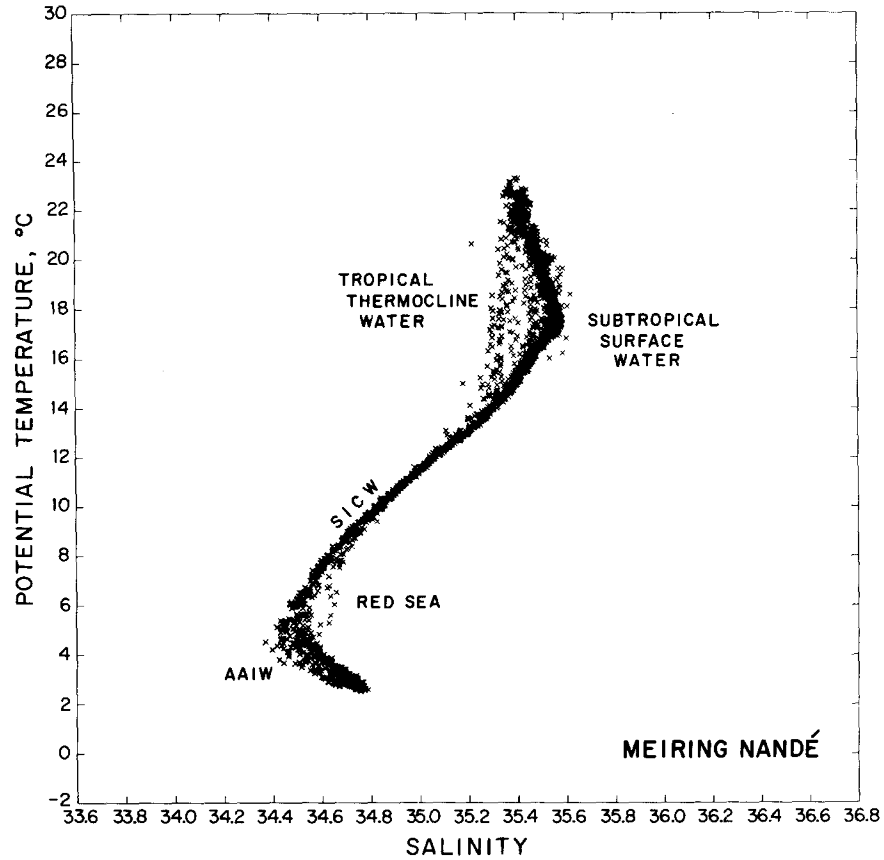

Fig. 9. Potential temperature vs salinity for the *Meiring Naude* data. Same water mass abbreviation as used in Fig. 8a.

At the base of the SICW is the salinity minimum of AAIW. The large range of salinity values within the density interval indicates some influence of the salty Red Sea water. The Red Sea influence is quite weak compared to the salinity levels further north; however the Red Sea influence can be considered at least as a "trace" or remnant. GRÜNDLINGH (1985) presents evidence of a Red Sea intrusion centered at the sigma-θ 27.35 within the Mozambique Basin. He traces it from the Mozambique Channel. Wyrtki's Red Sea core layer maps (Plates 282–287) clearly show the salty Red Sea water spreading southward within the Mozambique Channel from the tropical western Indian Ocean.

Water masses—R. V. Knorr *data set*

The stations which define the Agulhas Current inflow, according to the baroclinic structure, are Stas 49 and 50. These are used in this capacity to inspect the *Knorr* data set for signs of water mass alteration within the Agulhas Retroflection. The θ–S relation for these stations (Fig. 10) is essentially identical with the *Meiring Naude* θ–S relationship. The tight curve associated with the SICW and the greater range of salinity within the water warmer than 15°C and within the AAIW interval reflect the same conditions discussed in regard to the *Meiring Naude* data set.

Salinity within the deep salinity maximum core layer is closer to that of the NADW than to the Indian Deep Water. This indicates that Indian Deep Water does not enter the Retroflection region (as further supported by the θ–O_2 relation for the full *Knorr* data set, discussed below).

The θ–O_2 curves for Stas 49 and 50 (Fig. 10) show structure consistent with the interpretation of the θ–S relation. The high oxygen of the SAMW embedded within the SICW is clearly revealed near the 12°C isotherm. The low oxygen layers near 15–17°C and near 4°C, mark the northern tropical thermocline and Red Sea waters, respectively. The shallower, warmer low oxygen minimum feature extends from 100 to 150 m at Stas 48, 49, 52 and 55 (Camp *et al.*, 1986). It is associated with the warm surface water of the axis of the Agulhas Current and Agulhas Return Current. This is the case for nearly every *Knorr* crossing of the Agulhas axis within the main Retroflection and within the Cape Town Eddy (e.g. Stas 13, 42, 45, 47, 65, 75, and 80; Camp *et al.*, 1986). In contrast, the Retroflection Eddy does not exhibit the shallow oxygen minimum, suggesting that

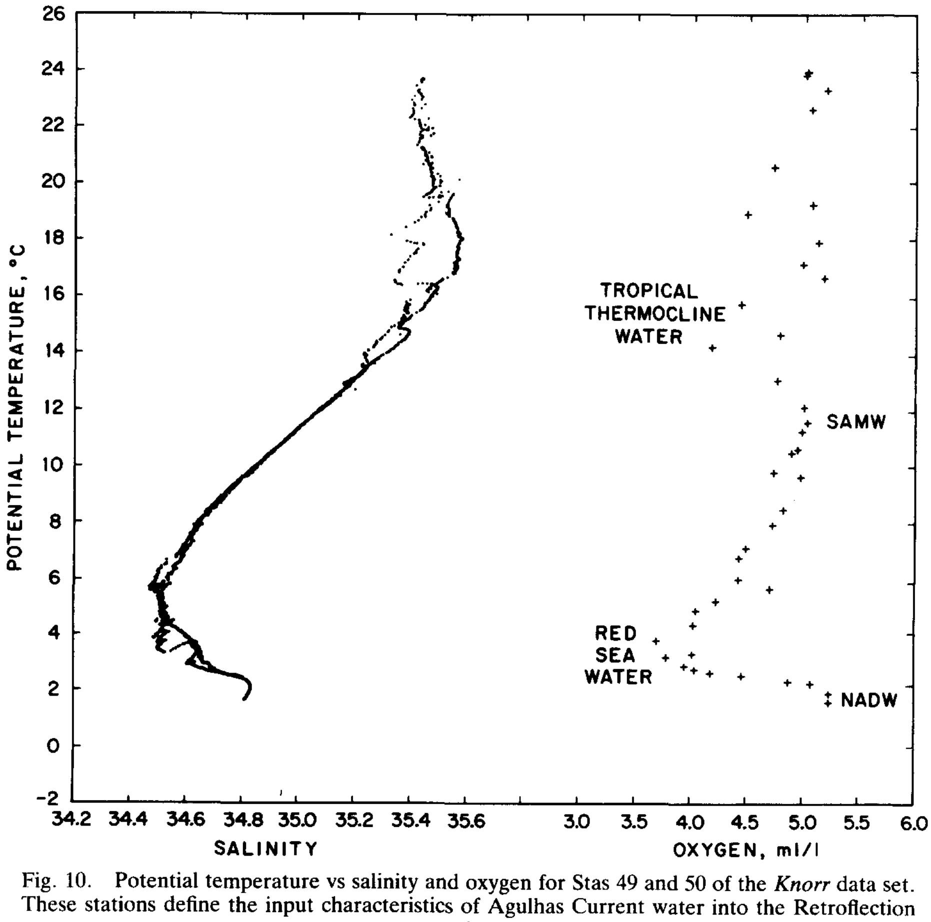

Fig. 10. Potential temperature vs salinity and oxygen for Stas 49 and 50 of the *Knorr* data set. These stations define the input characteristics of Agulhas Current water into the Retroflection region.

the ring of Agulhas Current water has been destroyed, perhaps not being directly renewed, as also is suggested by the absence of a warm surface water ring.

The AAIW oxygen is not as high as that associated with this water mass further east (see, for example, the salinity minimum core layer maps of W-71, Plates 288–294); this is expected in that the western boundary region is affected by "older" AAIW flowing in from the north. In addition this AAIW would have mixed with the low oxygen, high salinity Red Sea water.

The full *Knorr* data set within the Retroflection region (Figs 11a,b) displays a much broader range of salinity at nearly every isotherm relative to the Agulhas input characteristics (Fig. 10). The input stations 49 and 50 fall to the high salinity side of the θ–S distribution at all temperatures except for a few points warmer than the 13°C isotherm (+δS in Fig. 11a), where the water in the Retroflection region is more saline by about 0.1. Relatively low salinity (–δS in Fig. 11a) is particularly evident in the AAIW interval, between 9 and 10°C and in the lower SICW, 11–14°C. The positive and negative salinity anomalies relative to the input stations 49 and 50 are induced either by interaction with the local atmosphere or by intrusions of Atlantic Water; these factors are discussed in Section 4.

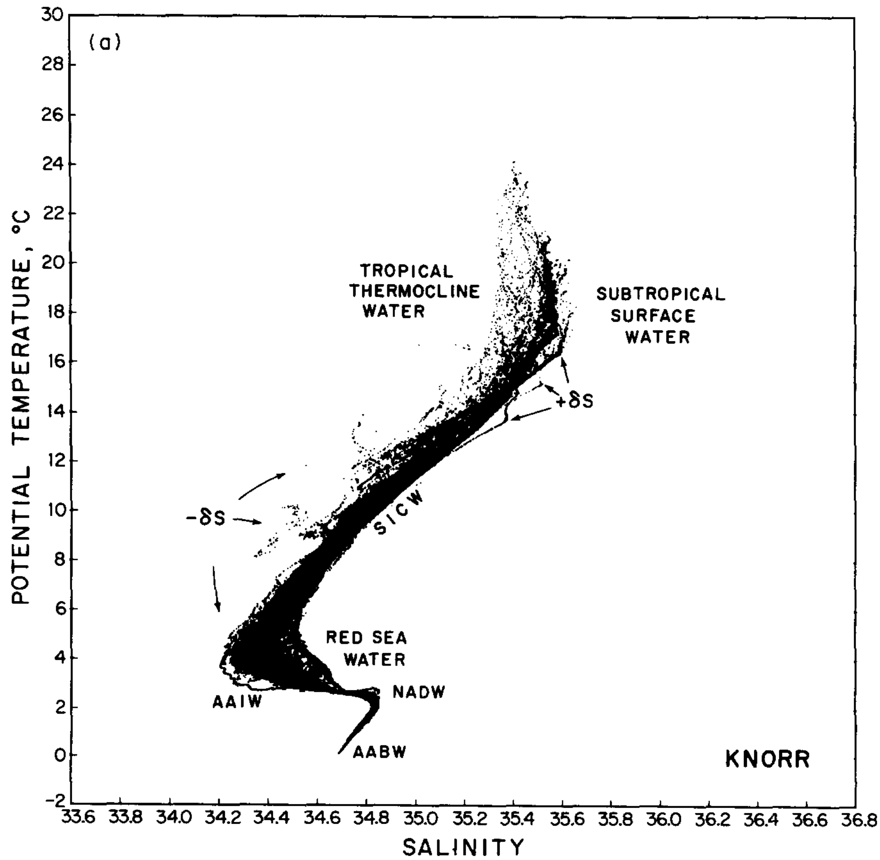

Fig. 11a.

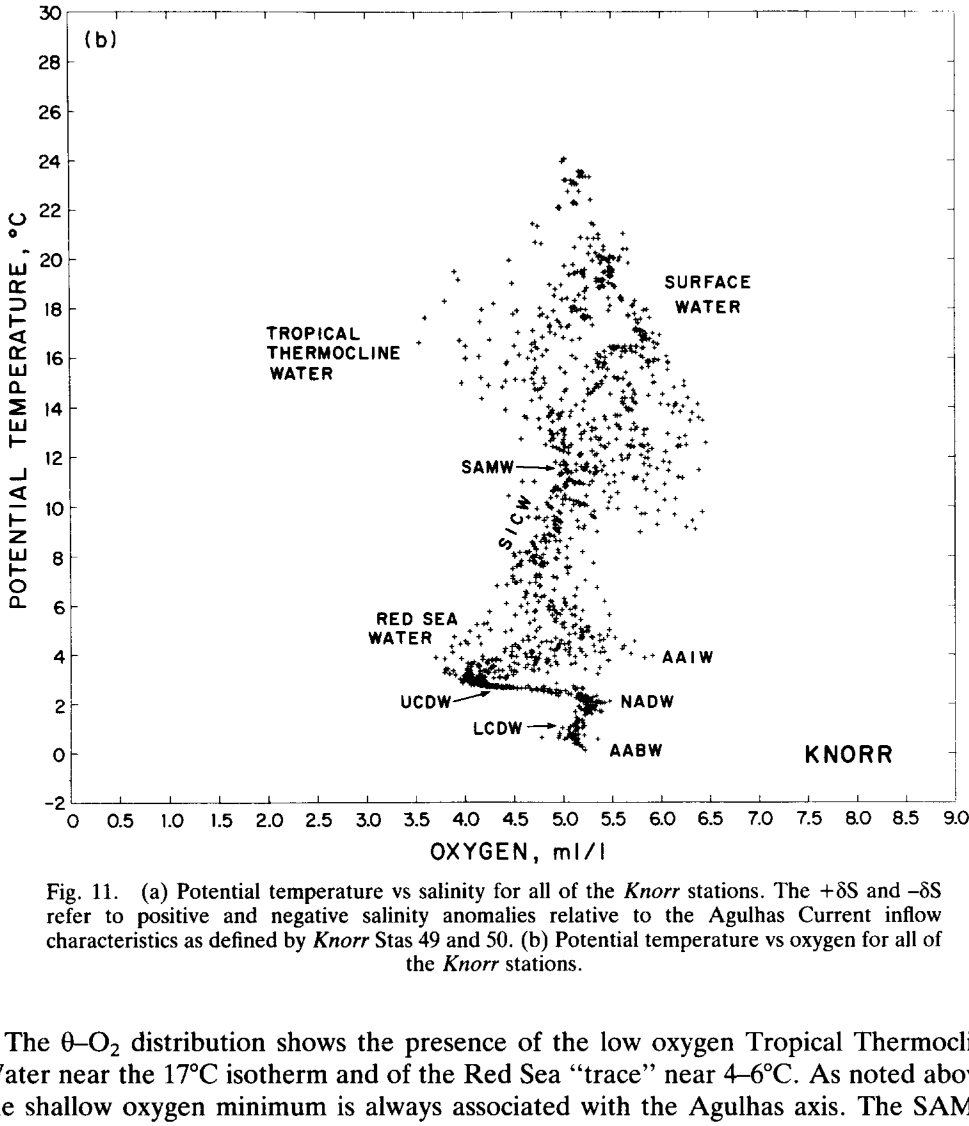

Fig. 11. (a) Potential temperature vs salinity for all of the *Knorr* stations. The $+\delta S$ and $-\delta S$ refer to positive and negative salinity anomalies relative to the Agulhas Current inflow characteristics as defined by *Knorr* Stas 49 and 50. (b) Potential temperature vs oxygen for all of the *Knorr* stations.

The θ–O_2 distribution shows the presence of the low oxygen Tropical Thermocline Water near the 17°C isotherm and of the Red Sea "trace" near 4–6°C. As noted above, the shallow oxygen minimum is always associated with the Agulhas axis. The SAMW marks an oxygen maximum between the two tropical inputs, but within the Retroflection the SAMW displays much higher oxygen concentrations than within the Indian Ocean thermocline. The Retroflection SAMW oxygen values are too high to be derived from the Agulhas input via Agulhas Passage. This water is associated with the relatively low salinity water (the $-\delta S$ features shown in Fig. 11a) which is derived, presumably from south of the Retroflection.

Below the AAIW and Red Sea "trace" stratum is the NADW and, as seen in the θ–O_2 distribution (Fig. 11b), the upper and lower CDW. At the sea floor is the AABW. The NADW salinity and oxygen concentration is somewhat above that of the interior of the Indian Ocean (Figs 8a, b). The salinity maximum core layer maps presented by W-71 (Plates 296–299) also indicate more concentrated NADW characteristics within the southwest corner of the Indian Ocean. In addition, there is no evidence that Indian Deep

Water with its low oxygen characteristics and absence of CDW components, enters the Agulhas Retroflection. This isolation occurs below the AAIW layer, in the sigma-θ 27.5–27.7 range (sigma-2 of 36.6 and 36.8), approximately at the 1500–2000 m level.

4. THERMOHALINE ALTERATION WITHIN THE AGULHAS RETROFLECTION

As mentioned in the previous section there are indications, particularly in the salinity data, of significant thermohaline modifications of the Indian Ocean Water once within the Agulhas Retroflection. For temperature above 13°C, there is water within the Retroflection displaying strong positive salinity anomalies, relative to the Agulhas inflow characteristics, defined as those of *Knorr* Stas 49 and 50; at lower temperatures the anomalies are all highly negative.

The anomalies are revealed in θ–S space (Fig. 11a) and on maps of salinity differences relative to the Agulhas inflow stations, as measured along density surfaces (Figs 12a–d). The positive salinity anomalies are most likely products of local atmospheric cooling of the upper thermocline, since there is no ocean source. This is the case for other regions where warm-core rings are spawned from western boundary regimes and drift into regions of strong cooling (OLSON *et al.*, 1985; SCHMITT and OLSON, 1985; GORDON, 1981; ROCHFORD, 1983). The low salinity anomalies are most intense in the southern and western areas of the station array and are likely to have been derived from intrusions of South Atlantic Water. The South Atlantic Water represents a transitional zone of the South Atlantic which is formed from a blend of thermocline water and Subantarctic Surface Water (perhaps formed within the Brazil-Falkland Confluence region, GORDON, 1981). The Atlantic Water enters the Agulhas Retroflection from the south, swept into the Retroflection region to the east of each of the Agulhas rings, and not from the Agulhas Current flow through the Agulhas Passage.

The salinity differences on the sigma-θ 26.0 surface (Fig. 12a), which lies at a position slightly deeper than the subtropical salinity maximum of the South Indian Ocean, show negative anomalies along the inshore Agulhas extending to deeper water immediately west of the separation into the Retroflection. This represents the lower salinity thermocline water associated with the shallow oxygen minimum, which hugs the inshore side of the Agulhas and which can be traced to tropical Indian Ocean source as discussed in the previous section. Within both the main Retroflection and Retroflection Eddy the anomalies are about zero. Positive salinity anomalies of over +0.10 are confined to the core of the Cape Town Eddy. This anomaly is represented consistently by all of the stations within the eddy core. Positive salinity anomalies are also observed on the 26.0 sigma-θ surface by *Meiring Naude* Stas 6 and 27 in the western part of the *Meiring Naude* grid and by *Meiring Naude* Sta. 42. These *Meiring Naude* points are isolated finer scale intrusions and do not represent distinct features. However, as discussed below, it is possible they represent some highly altered water derived from the Agulhas Retroflection.

The southwest extreme of the *Knorr* grid (Sta. 23) displays the largest negative salinity anomalies. The stations neighboring Sta. 23 also display large negative anomalies, which define the extent of the South Atlantic influence into the Agulhas system.

The sigma-θ 26.5 (Fig. 12b), associated with the upper thermocline, displays near-zero salinity anomaly within the *Meiring Naude* grid, within the main Retroflection, Retroflection Eddy and Cape Town Eddy, indicating no modification. Negative salinity

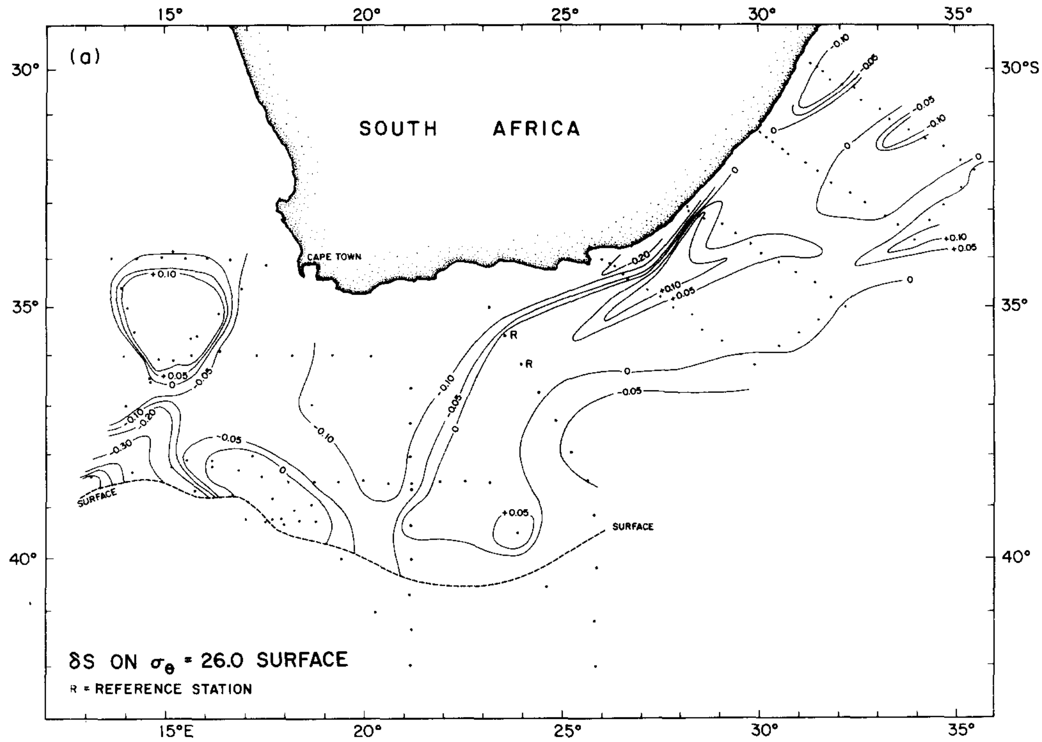

(a)
SOUTH AFRICA
CAPE TOWN
SURFACE
R
δS ON σ_θ = 26.0 SURFACE
R = REFERENCE STATION
15°E
20°
25°
30°
35°
30°S
35°
40°

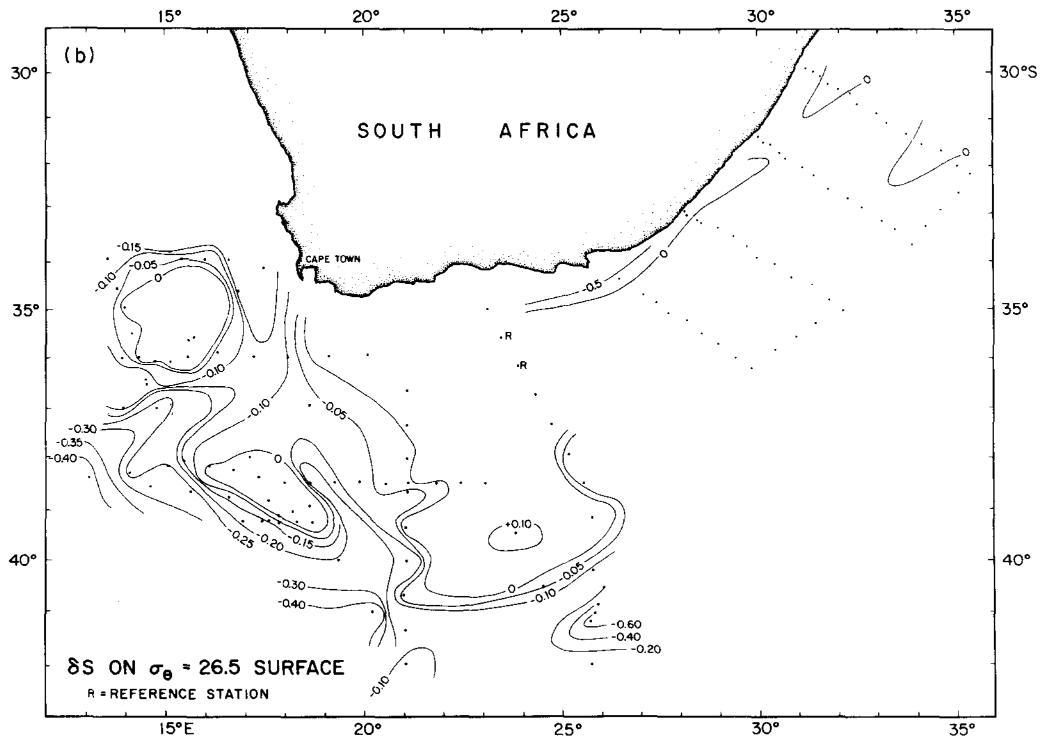

(b)
SOUTH AFRICA
CAPE TOWN
R
δS ON σ_θ = 26.5 SURFACE
R = REFERENCE STATION
15°E
20°
25°
30°
35°
30°S
35°
40°

Figs 12a,b.

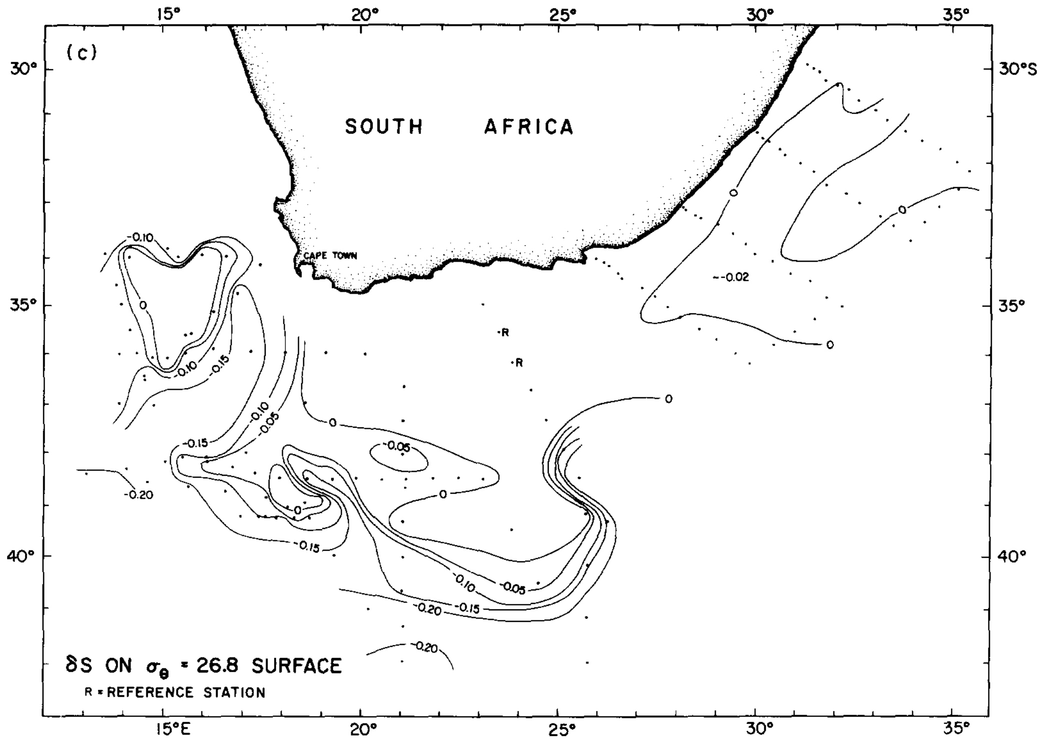

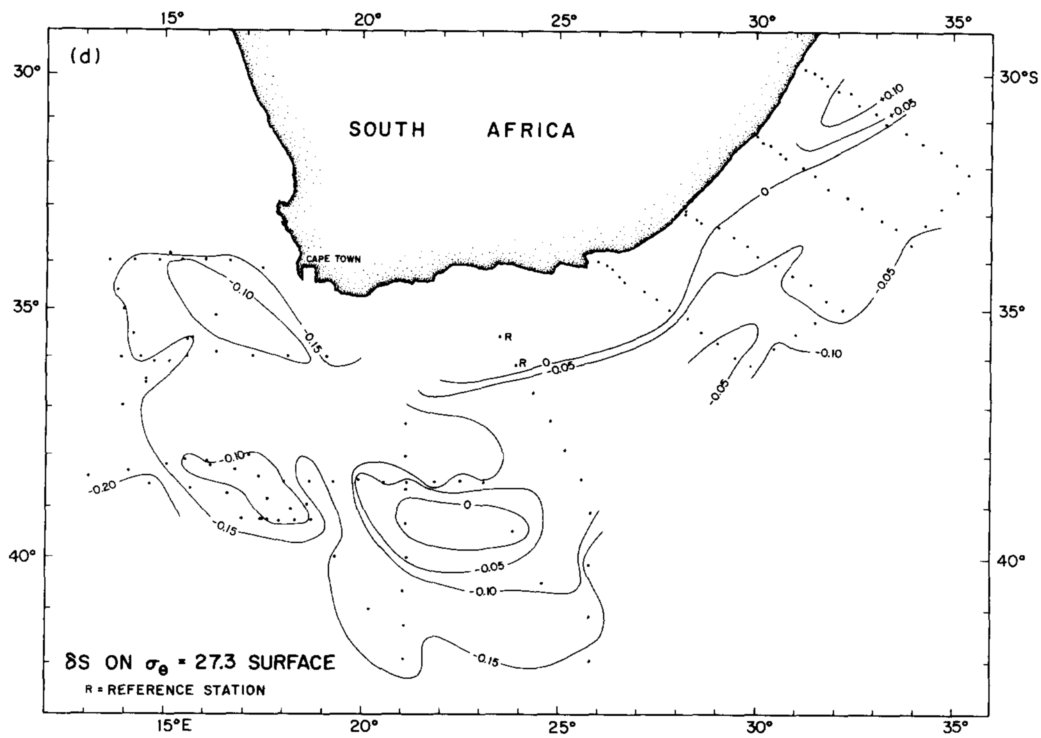

Fig. 12. (a) Salinity anomaly on the sigma-θ 26.0 surface. These are determined by differencing the salinity at each *Knorr* station to the averaged salinity value of *Knorr* Stas 49 and 50 at 26.0 sigma-θ. Stations 49 and 50 represent the Agulhas Current characteristics which enter the Retroflection region. (b) Same as (a), except for sigma-θ 26.5. (c) Same as (a), except for sigma-θ 26.8. (d) Same as (a), except for sigma-θ 27.3.

anomaly is observed to invade into the remainder of the station array to a greater extent than is the case with the shallower 26.0 sigma-θ isopycnal. The South Atlantic Water represented by Sta. 23, has a negative anomaly of 0.40. The influence of this water in depressing salinity is seen as negative anomalies of 0.20 spread into the Agulhas system to the south and east of the two eddies. Within the southeast corner of the *Knorr* grid (Sta. 57) the negative anomaly attains –0.60 suggesting intrusion of more southern water into the system, carried in by the anticyclonic eddy found at Sta. 58.

The sigma-θ surface 26.8 (Fig. 12c) within the lower thermocline again shows near-zero salinity anomalies within the *Meiring Naude* grid, main Retroflection, Retroflection Eddy and Cape Town Eddy. Thus Indian Ocean Water is preserved within these features of the Agulhas Retroflection system. The negative salinity anomalies marking the South Atlantic "contamination" are drawn into the Retroflection system by the two eddies, as also seen at the shallower isopycnal surfaces, in a manner consistent with the associated anticyclonic circulation.

At the AAIW sigma-θ 27.3 level (Fig. 12d), the salinity anomalies are mostly within 0.20 of the reference stations. The positive anomaly entering at the northern-most *Meiring Naude* section marks input of Red Sea remnants. The main Retroflection core is near zero anomaly, so it has not been "contaminated" by South Atlantic Water. The two eddies have been affected at the AAIW level by South Atlantic Water, as indicated by anomalies of –0.10. The Agulhas Return Current has negative salinity anomalies both in the *Knorr* and in the *Meiring Naude* grids, indicating that this current carries Atlantic AAIW characteristics into the South Indian subtropical gyre.

Positive salinity anomalies

The warm Indian Ocean Water advected into the Retroflection region is exposed to a relatively cold atmosphere and hence experiences significant cooling (Bunker, 1980). An important term in the heat loss is the evaporation, though it is noted that cooling alone would produce a mixed layer which stands out as a positive salinity anomaly relative to the initial input thermocline θ–S curve. The altered mixed layer would follow the regional θ–S curve only if sufficient precipitation is introduced. Positive salinity anomaly would be induced if:

$$Q/s_0F > \mathrm{d}\theta/\mathrm{d}S,$$

where Q is the heat loss to the atmosphere; s_0 in the initial salinity; F is the net fresh water input to the ocean and $\mathrm{d}\theta/\mathrm{d}S$ is the thermocline curve (see Gordon, 1981). With a large Q, as expected for the Retroflection region, F must be large to suppress a positive salinity anomaly. Thus it is proposed that the positive salinity anomalies are products of local cooling. Furthermore the "parent" water mass which is locally modified is the subsurface salinity maximum near 18°C.

The *Knorr* stations which display the most intense subsurface positive salinity anomalies relative to the Agulhas input conditions (Stas 49 and 50) are within the main Retroflection and warm-core eddies: Stas 5 (core of the Cape Town Eddy), 39 (the eddy found just south of the Agulhas Return Current along 21E) and 60 (within the center of the main Retroflection; Fig. 13a). Anomalies amount to slightly greater than 0.10. The Retroflection Eddy does not display any positive salinity anomalies. The positive salinity anomalies are associated with increased oxygen concentrations, relative to the Agulhas input characteristics (Fig. 13b) by nearly 1.0 ml l^{-1}. These anomalies are associated with pycnostads (Fig. 14; Table 1).

Within the main Retroflection and Retroflection Eddy is a pycnostad with a temperature just below 18°C (Stas 61–63 and 70–72 in Fig. 5). This water type marks the salinity maximum of the Subtropical Water discussed in Section 3; it is not a positive salinity anomaly relative to the input stations (though it is relative to the Tropical Thermocline component). The thickness of the 17–19°C water layer (Fig. 15) shows the geographic extent of this layer. There is a maximum thickness within the main Retroflection and Retroflection Eddy. In view of the large heat losses to the atmosphere in this region, it is possible that the pycnostad is exposed directly to the atmosphere during the winter period. The *Knorr* data within the Retroflection Eddy (Fig. 5) indicate that in December, a period of maximum incoming solar radiation, this layer is nearly exposed to the atmosphere (e.g. Sta. 71 with a surface temperature and salinity of 18.87°C and 35.58, respectively). A maximum thickness is also observed in the *Meiring Naude* grid, within the central part of the anticyclonic circulation pattern. While it also could be produced locally, it is more likely that it represents an outflow from the main Retroflection. In any case it is probable that the 18°C pycnostad represents a remnant winter mixed layer, and

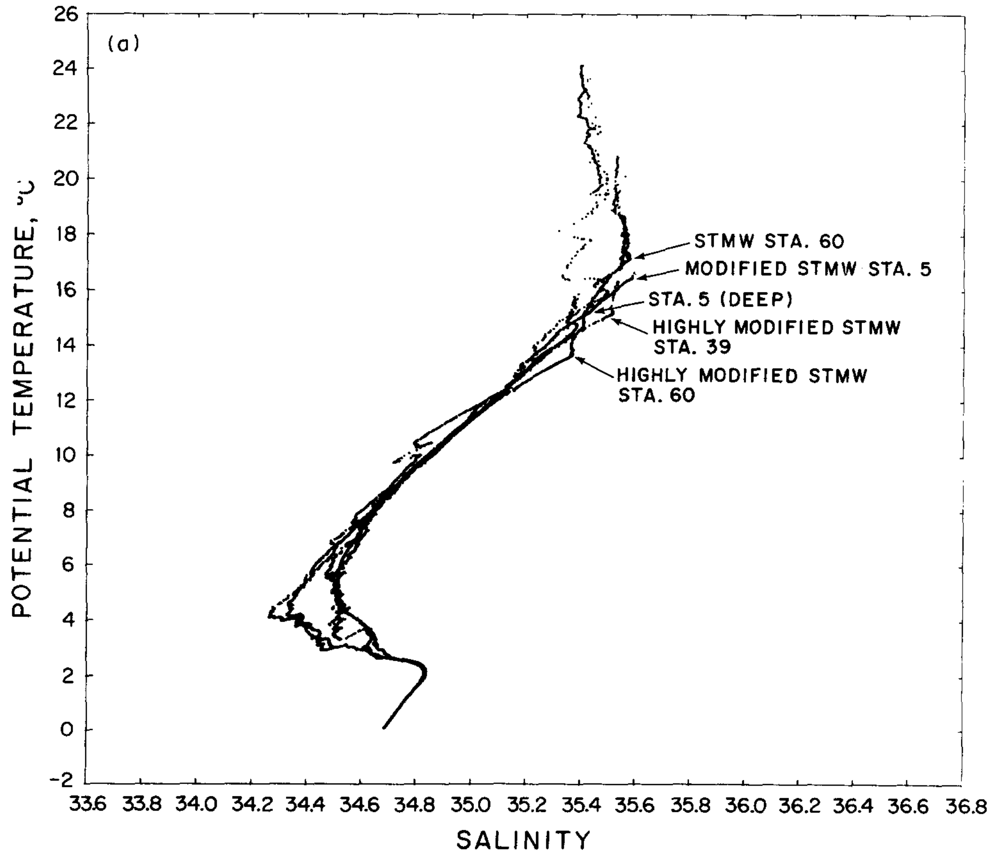

Fig. 13a.

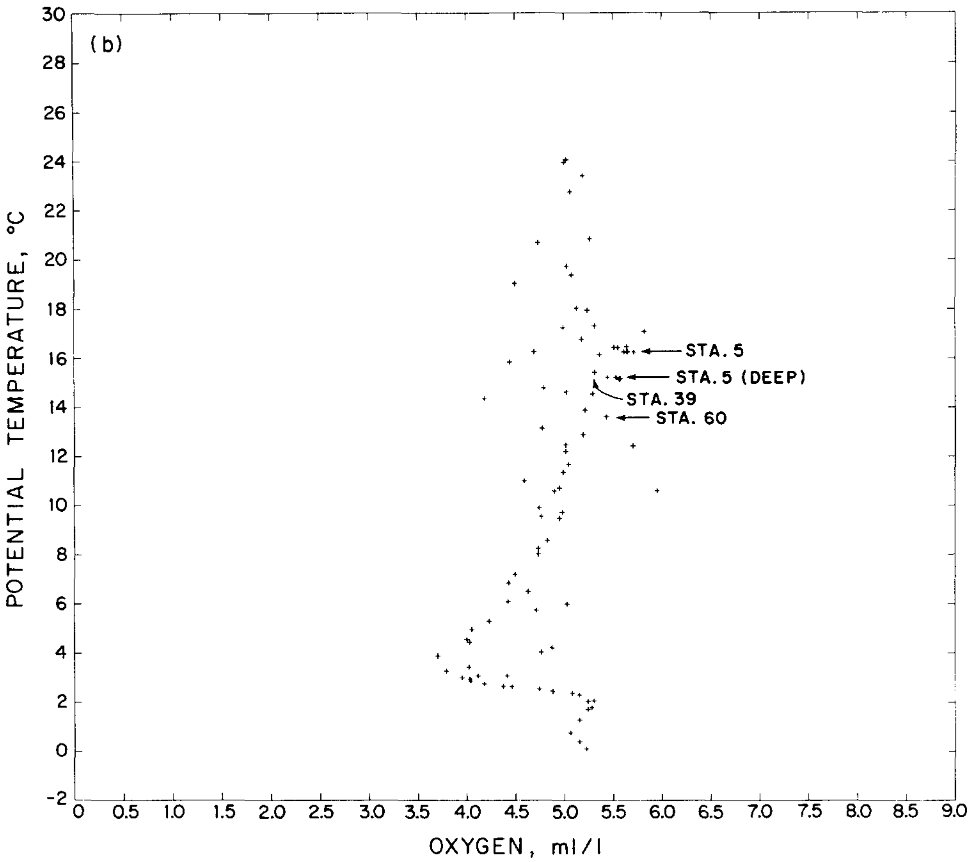

Fig. 13. (a) Potential temperature vs salinity for a selection of *Knorr* stations displaying positive salinity anomalies. (b) Potential temperature vs oxygen for same stations as used in (a).

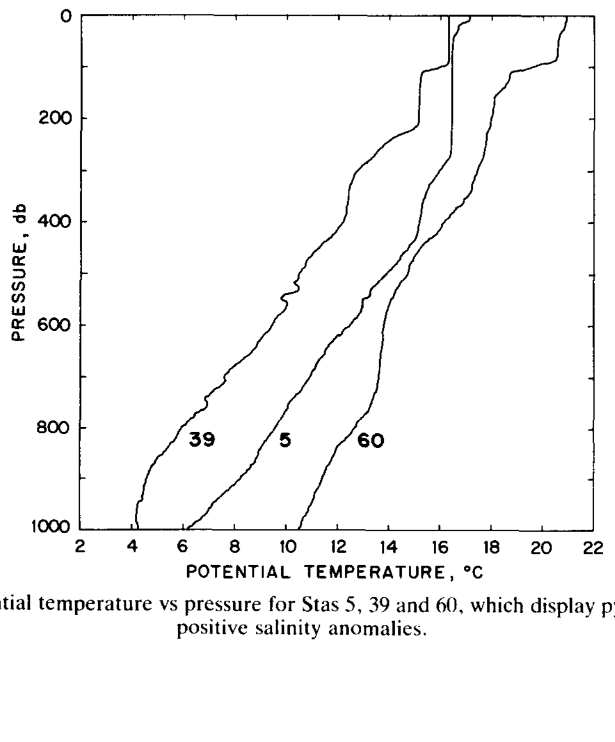

Fig. 14. Potential temperature vs pressure for Stas 5, 39 and 60, which display pycnostads with positive salinity anomalies.

Table 1. Characteristics of the positive salinity anomaly pycnostads

Station	Depth (m)	Temperature (°C)	Salinity
5	40–265	16.4	35.58
5	370–420	15.2	35.43
39*	105–205	15.1	35.51
60	600–725	13.6	35.36
For reference (see Sta. 60):			
STMW†	160–300	17.8	35.56

* At Sta. 39 there is a deeper pycnostad between 300 and 400 m with a temperature–salinity value of 12.3–35.12; it does not stand out as a positive salinity anomaly, and hence is not included in this discussion. Its origin may lie in the South Atlantic.

† Subtropical Mode Water.

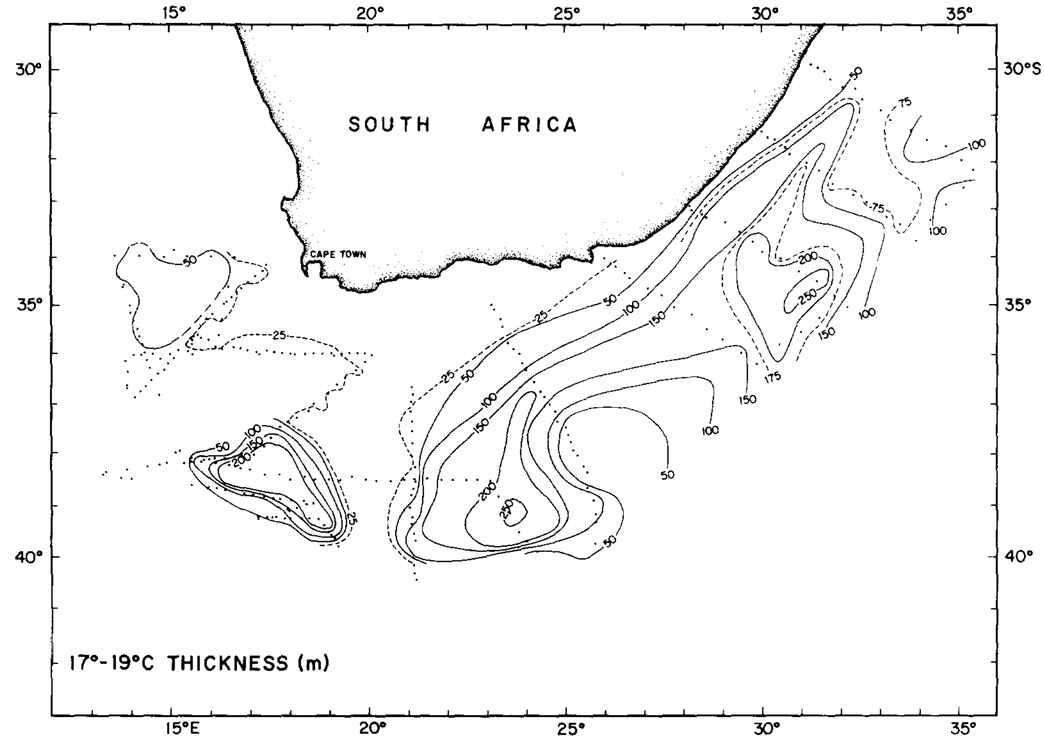

Fig. 15. Thickness (meters) between the 17 and 19°C isotherms.

as such could be called the Subtropical Mode Water (STMW). Whether this water is responsible for the entire subtropical subsurface salinity maximum of the South Indian Ocean is an interesting possibility.

The thickness of the 15–17°C layer (Fig. 16) clearly shows the colder pycnostad within the Cape Town Eddy and the eddy at Sta. 39.

It is proposed that the pycnostads seen at Stas 5, 39 and at depth in the thermocline at Sta. 60 represent altered STMW. This alteration occurs within the warm-core rings of the Agulhas Retroflection. Furthermore, the double occurrence of pycnostads marked with

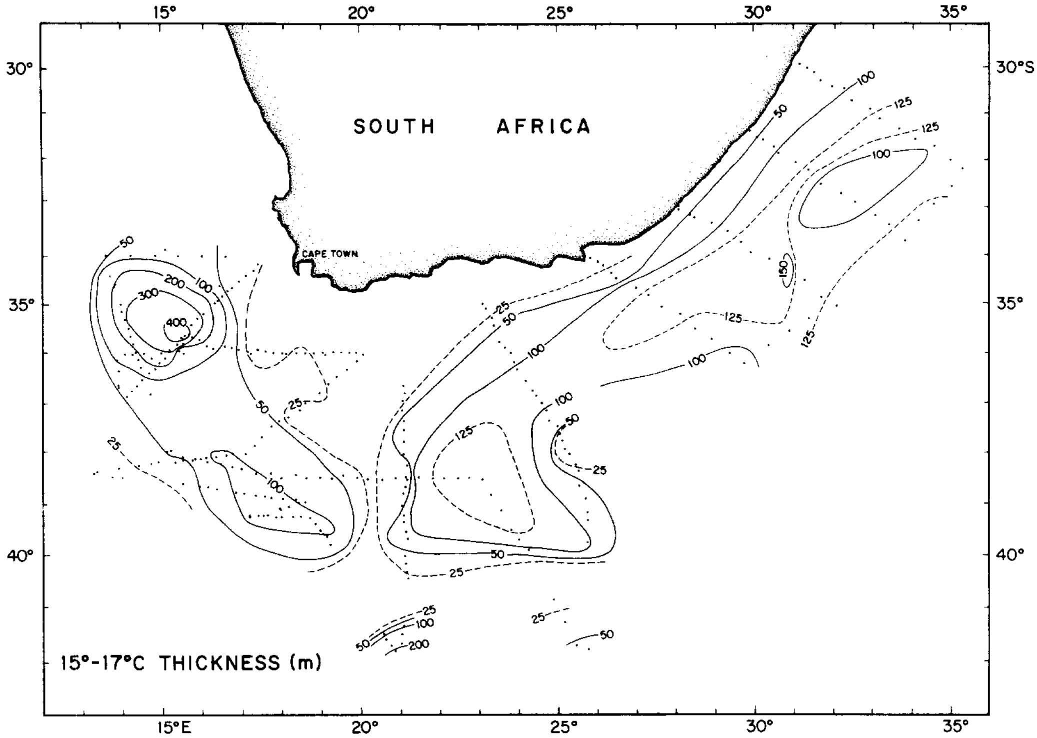

Fig. 16. Thickness (meters) between the 15 and 17°C isotherms.

positive salinity anomalies indicates that pools of water, which have been altered to a cooler, denser state than the STMW "parent" water type, are re-absorbed by the main Retroflection (e.g. Sta. 60) or by other rings (e.g. the deeper "stad" at Sta. 5), to ventilate water layers at depth. This process has been reported for the Gulf Stream system (SCHMITT and OLSON, 1985) and for the Brazil Current System (GORDON, 1981); coalescence of two warm-core eddies has been documented in the East Australian Current regime (CRESSWELL, 1983). In the case of Sta. 60, there is a significant effect on the baroclinic field, in that these stads would enhance the anticyclonic feature centered at Sta. 60.

The presence of Agulhas derived warm-core eddies to the west (Retroflection Eddy), to the northwest (Cape Town Eddy) and to the south (the Sta. 39 feature) of the main Retroflection and the evidence of absorption of eddies by the main Retroflection, indicates the extent of these features and their effect on ventilation of the thermocline. The *Knorr* data suggest that warm-core eddies spawned from the Agulhas Retroflection can either drift and decay within the South Atlantic or drift back into the Indian Ocean and possibly be re-absorbed by the Agulhas Retroflection.

Negative salinity anomalies

The negative salinity anomalies are greatest exterior to the main Retroflection and warm-core eddies (Fig. 12). In the upper thermocline (sigma-θ of 26.0, Fig. 12a) anomalies in excess of −0.20 are confined to the southwest corner of the *Knorr* grid. As depth and density increase, the negative anomalies invade further into the Retroflection region, following a path along the edge of the two warm-core eddies. At the sigma-θ 27.3 surface, negative salinity anomalies are found throughout the region including the warm-core eddies (though the main Retroflection still has an area of zero anomaly). Basically, with increasing depth the water masses within the Retroflection region become more like those of the South Atlantic water masses. In addition, as mentioned in Section 3, at depths below the intermediate water layer there is no Indian Ocean Water within the Agulhas Retroflection.

Thus a picture emerges in which Indian Ocean Water enters the Agulhas Retroflection only at densities less than approximately sigma-θ of 27.5 (nominally 1500–2000 m), and that the Indian Ocean Water that does enter the Retroflection water becomes increasingly "contaminated" with South Atlantic Water, as depth increases. The baroclinic geostrophic transport (Fig. 7) indicates that about one third of the transport into the South Atlantic within the upper 1500 m associated with the Agulhas branch, is derived from the South Atlantic, giving a quantitative value for the net amount of contamination.

The θ–S and θ–O_2 grouping for stations displaying strong negative salinity anomalies (Figs 17a,b) fall between the Agulhas input Stas 49 and 50 and Sta. 23, which marks the southwest corner of the *Knorr* grid. The elevated oxygen concentrations are particularly evident in the 3–7°C temperature range, where the Agulhas input, which is very low in

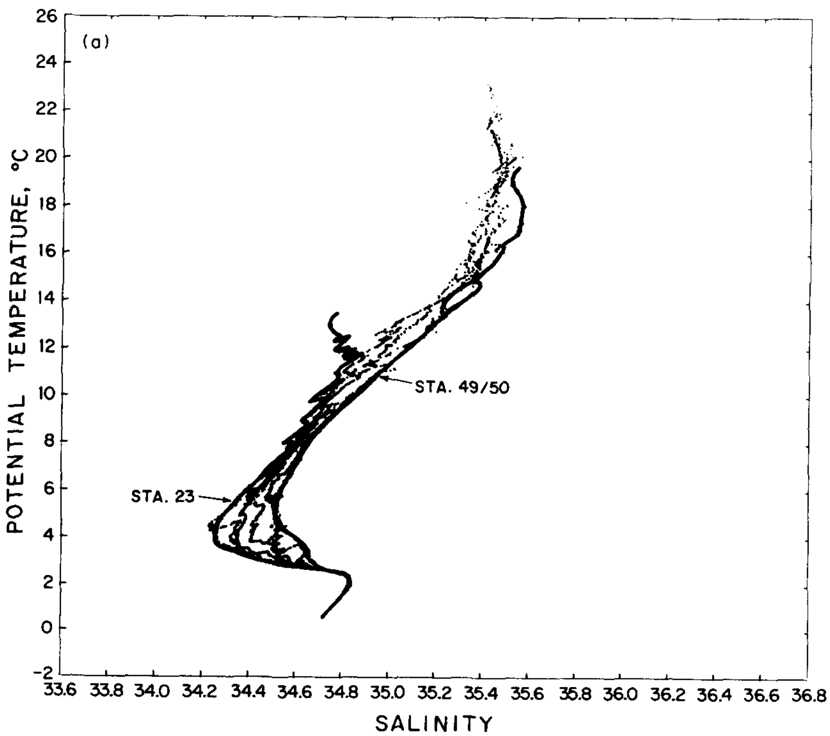

Fig. 17a.

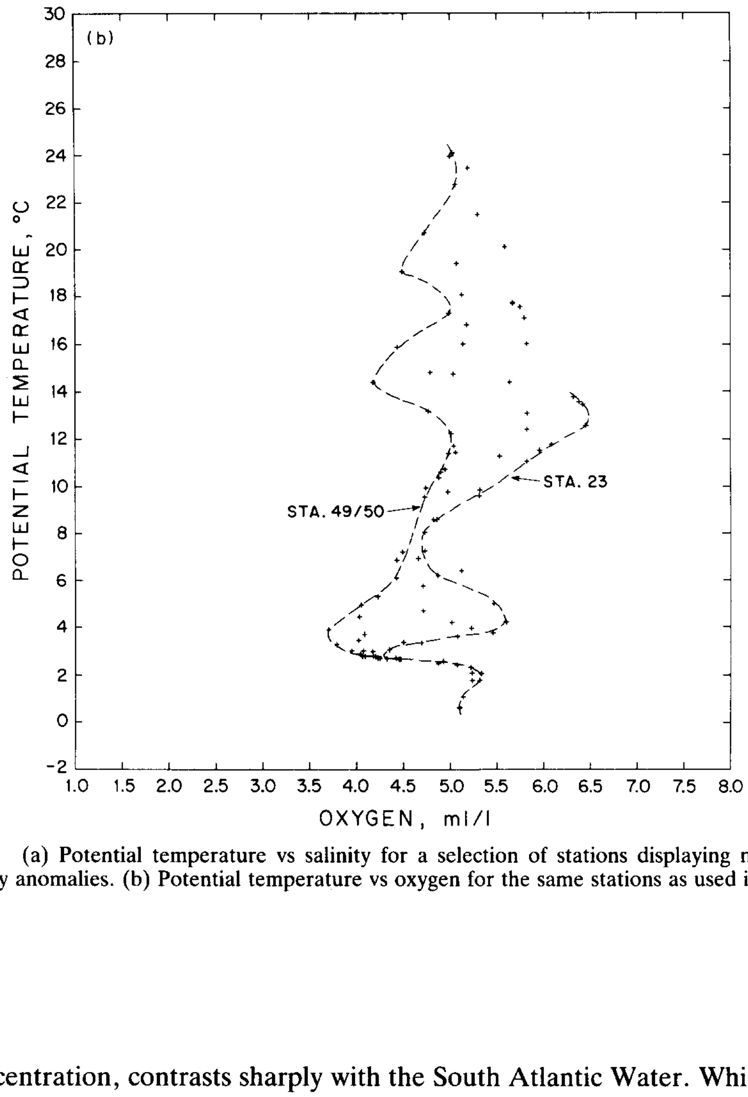

Fig. 17. (a) Potential temperature vs salinity for a selection of stations displaying negative salinity anomalies. (b) Potential temperature vs oxygen for the same stations as used in (a).

oxygen concentration, contrasts sharply with the South Atlantic Water. While the trend towards lower salinity and higher oxygen occurs at all levels below sigma-θ 26.5, there is a minimum in this effect near sigma-θ 27.0. This is due to a reduced contrast between the Indian and South Atlantic oceans at that density horizon (Gordon, 1985).

The South Atlantic circulation (Tsuchiya, 1985) is directed to the east of latitude south of 30°S. The θ–S properties for the latitudes from 30° to 44°S along the greenwich meridian (Fig. 18), as measured from *Knorr* during the AJAX program (SIO Data Report, 1985) just prior to the Agulhas cruise, reveal the Atlantic Water, particularly in the 40°–44°S band, is very similar to that observed at Sta. 23. Therefore it is reasonable to conclude that the source of the low salinity water mixing into the Agulhas Retroflection is derived from the South Atlantic south of 30°S. Within this belt the South Atlantic is a blend of thermocline water with the colder fresher Subantarctic Surface Water which entered the Atlantic via the Drake Passage (also see the property-property plots in the Southern Ocean Atlas, Gordon and Molinelli, 1982).

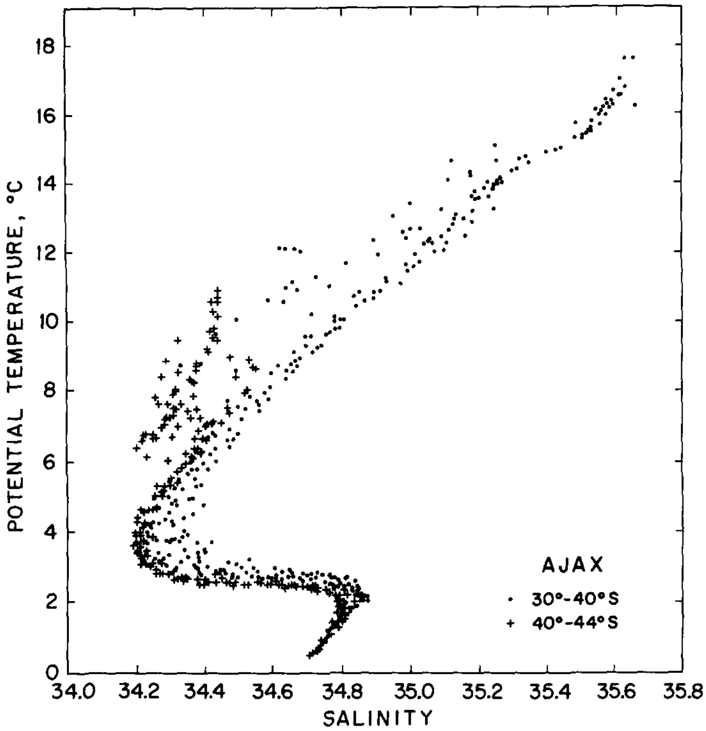

Fig. 18. Potential temperature vs salinity for the AJAX stations between 30° and 44°S.

5. CONCLUSIONS

The October–December 1983 characteristics of the Agulhas Retroflection region, as observed by the R.V. *Knorr* and R.V. *Meiring Naude*, involve energetic circulation and a melange of water masses. Within the Agulhas Retroflection two such diverse water masses as Indian Ocean tropical and remnants of subantarctic water merge.

The principal results of the study are as follows:

(1) Within the upper 1500 m, the Agulhas Current introduces about 70 Sv of water (relative to 1500 db) into the Agulhas Retroflection (95 Sv relative to the sea floor). A small part of this flow, about 10 Sv, combines with 5 Sv of South Atlantic Water (which is derived from a blend of South Atlantic thermocline and subantarctic water) to flow into the South Atlantic. Most of the Agulhas Current transport returns to the Indian Ocean as the current undergoes a sharp retroflection along 21°E, after separation from the African continental margin. The Retroflection position observed in late 1983 falls at the eastern-most limits of its range, as reported in satellite i.r. studies.

(2) To the west of the Agulhas Retroflection are two warm-core eddies which have been spawned at the Agulhas Current. The eddy immediately west of the Retroflection, called the Retroflection Eddy, has an ellipitical form with minor and major diameters of 100 and 250 km, respectively, and a characteristic transport of 40 Sv. Its core properties are nearly identical to that of the main Retroflection. It is likely that the Retroflection

Eddy was spawned just prior to the cruise. The older, more circular eddy, referred to as the Cape Town Eddy, with a diameter of 200 km, has a characteristic transport of 35 Sv. It's core properties have been significantly altered by the local atmosphere from the source water characteristics within the main Retroflection.

(3) The Agulhas Current introduces several Indian Ocean Water types into the Agulhas Retroflection region. These include water from the: (a) South Indian Ocean subtropical thermocline water, which includes a form of Subantarctic Mode Water; (b) tropical thermocline from the western Indian Ocean; (c) saline, low oxygen remnants of Red Sea water within the density range of the lower thermocline; (d) Antarctic Intermediate Water.

There are no signs that Indian Ocean Water, with density greater than sigma-θ of 27.5–27.7, enters the Retroflection. It is probable that Indian Ocean Deep Water is absent from a somewhat more extensive region of the southwest Indian Ocean. Thus, while the Agulhas Retroflection circulation pattern may extend to greater densities, at densities greater than sigma-θ 27.5 (below a depth of 1500–2000 m) the Retroflection is composed of South Atlantic and circumpolar water.

(4) Within the Agulhas Retroflection Indian Ocean water masses are modified in two ways: (a) The upper thermocline water upon exposure to the colder atmosphere forms water which is anomalously salty relative to the Agulhas inflow. This water is confined for the most part within the cores of the main Retroflection and the warm eddies. (b) The deeper thermocline water mixes with South Atlantic Water which enters the Retroflection region by being swept in with the anticyclonic circulation of the warm-core eddies. The "contamination" of the Agulhas Retroflection thermocline with South Atlantic Water increases with depth, until density levels are reached at which no contribution from the Indian Ocean is evident.

Both these alterations are associated with elevated oxygen concentrations.

Acknowledgements—The support for the R.V. *Knorr* cruise and the associated processing and data analysis of ALG was supported by N000-14-84-C-0132. The support of the technical staff and crew of the *Knorr* and *Meiring Naude* is gratefully acknowledged. Lamont-Doherty Contribution no. 4098.

REFERENCES

Bang N. D. (1970) Dynamic interpretations of a detailed surface temperature chart of the Agulhas Current retroflexion and fragmentation area. *South African Geographical Journal*, **52**, 67–76.

Bang N. D. (1973) Characteristics of an intense ocean frontal system in the upwelling regime west of Capetown. *Tellus*, **25**, 256–265.

Bang N. D. and W. R. H. Andrews (1974) Direct current measurements of a shelfedge frontal jet in the Southern Benguela System. *Journal of Marine Research*, **32**, 405–417.

Bennett S. L., J. R. Luyten and J. M. Toole (1985) The Agulhas and Agulhas return currents: Analysis of CTD/O_2 sections crossing the currents and an XBT survey following the 15°C at 200 m contour. Abstract *EOS*, **66**, 930.

Bunker A. F. (1980) Trends of variables and energy fluxes over the Atlantic Ocean from 1948 to 1972. *Monthly Weather Review*, **108**, 720–728.

Camp D., W. Haines, B. Huber, S. Rennie and A. Gordon (1986) Agulhas retroflection cruise, November–December 1983. A Data Report, Lamont-Doherty Geological Observatory Technical Report, 86–1.

Cheney R. E., J. G. Marsh and B. D. Beckley (1983) Global mesoscale variability from collinear tracks of SEASAT altimeter data. **88**, 4331–4538.

Colborn J. G. (1975) *The thermal structure of the Indian Ocean.* University Press of Hawaii, Honolulu, 173 pp.

Colton M. T. and R. R. P. Chase (1983) Interaction of the Antarctic Circumpolar Current with bottom topography: An investigation using satellite altimetry. *Journal of Geophysical Research*, **88**, 1825–1843.

CRESSWELL G. R. (1983) Physical evolution of Tasman Sea Eddy J. *Australian Journal of Marine and Freshwater Research*, **34**, 495–513.
DARBYSHIRE J. (1972) The effect of bottom topography on the Agulhas Current. *Reviews of Pure and Applied Geophysics*, **101**, 208–220.
DE RUIJTER W. (1982) Asympototic analysis of the Agulhas Current. *Review of Pure and Applied Geophysics*, **12**, 361–373.
DIETRICH G. (1935) *Veroeffentlichungen der Internationalen Kommission fuer der Meer.* University of Berlin, Berlin, 27, p. 1.
DUNCAN C. P. (1968) An eddy in the subtropical convergence Southwest of South Africa. *Journal of Geophysical Research*, **73**, 531–534.
DUNCAN C. P. (1970) The Agulhas Current. PhD Thesis, University of Hawaii, 76 pp.
FU L. (1986) Mass, heat and freshwater fluxes in the south Indian Ocean. *Journal of Physical Oceanography*, **16**, in press.
GORDON A. L. (1981) South Atlantic thermocline ventilation. *Deep-Sea Research*, **28**, 1239–1264.
GORDON A. L. (1985) Indian–Atlantic transfer of thermocline water at the Agulhas retroflection. *Science*, **227**, 1030–1033.
GORDON A. L. (1986) Inter-ocean exchange of thermocline water. *Journal of Geophysical Research*, **91**, 5037–5046.
GORDON A. L. and E. M. MOLINELLI (1982) *The Southern Ocean Atlas: Thermohaline and chemical distributions and the Atlas data set.* Columbia University Press, New York, pp. 1–11; Plates 1–233.
GRÜNDLINGH M. L. (1977) Drift observations from Nimbus VI satellite-tracked buoys in the southwestern Indian Ocean. *Deep-Sea Research*, **24**, 903–913.
GRÜNDLINGH M. L. (1978) Drift of a satellite-tracked buoy in the southern Agulhas Current and Agulhas Return Current. *Deep-Sea Research*, **25**, 1209–1224.
GRÜNDLINGH M. L. (1980) On the volume transport of the Agulhas Current. *Deep-Sea Research*, **27**, 557–563.
GRÜNDLINGH M. L. (1983) On the course of the Agulhas Current. *South African Geographical Journal*, **65**, 49–57.
GRÜNDLINGH M. L. (1985) Occurrence of Red Sea Water in the southwestern Indian Ocean, 1981. *Journal of Physical Oceanography*, **15**, 207–212.
GRÜNDLINGH M. L. (1986) Features of the northern Agulhas Current in spring, 1983. *South African Journal of Science*, **82**, 18–20.
HAINES W. E., P. A. MELE, D. B. CAMP and S. E. RENNIE (1984) South Atlantic XBT Data 1979–1984. Lamont-Doherty Geological Observatory Technical Report, 84–4.
HARRIS T. F. W. (1972) Sources of the Agulhas Current in the spring of 1964. *Deep-Sea Research*, **19**, 633–650.
HARRIS T. F. W. and D. VAN FOREEST (1978) The Agulhas Current in March 1969. *Deep-Sea Research*, **25**, 549–561.
HARRIS T. F. W., R. LEGECKIS and D. VAN FOREEST (1978) Satellite infra-red images in the agulhas Current system. *Deep-Sea Research*, **25**, 543–548.
HELLERMAN S. and M. ROSENSTEIN (1983) Normal monthly wind stress over the world ocean with error estimates. *Journal of Physical Oceanography*, **13**, 1093–1104.
IVANENKOV V. N. and F. A. GUBIN (1960) Vodnye massy i gidrokhimiya zapadnoi i yuzhnoi chastei Indiiskogo okeana. *Trudy Morskogo Gidrofizicheskogo Instituta*, **22**, 33–115. (Water masses and hydrochemistry of the western and southern parts of the Indian Ocean. *Transactions of the Marine Hydrophysical Institute*, Academy of Sciences of the U.S.S.R., Physics of the Sea, Hydrology, **22**, 29–99.)
JACOBS S. S. and D. T. GEORGI (1977) Observations on the South-west Indian/Antarctic Ocean. In: *A voyage of discovery: George Deacon 70th anniversary volume*, Vol. 24, M. ANGEL, editor, Supplement to *Deep-Sea Research*, Pergamon Press, Oxford, pp. 43–84.
JOYCE T. M., R. W. SCHMITT and M. C. STALCUP (1983) Influence of the Gulf Stream upon the short-term evolution of warm-core ring. *Australian Journal of Marine and Freshwater Research*, **34**, 515–524.
LUTJEHARMS J. R. E. (1976) The Agulhas Current system during the northeast monsoon season. *Journal of Physical Oceanography*, **6**, 665–670.
LUTJEHARMS J. R. E. (1981a) Spatial scales and intensities of circulation in the ocean areas adjacent to South Africa. *Deep-Sea Research*, **28**, 1289–1302.
LUTJEHARMS J. R. E. (1981b) Features of the Southern Agulhas Current Circulation from satellite remote sensing. *South African Journal of Science*, **77**, 231–236.
LUTJEHARMS J. R. E. and H. R. VALENTINE (1984) Southern ocean thermal fronts south of Africa. *Deep-Sea Research*, **31**, 1461–1475.
LUTJEHARMS J. R. E. and R. C. VAN BALLEGOOYEN (1984) Topographic control in the Agulhas Current system. *Deep-Sea Research*, **31**, 1321–1337.
LUTJEHARMS J. R. E., N. D. BANG and C. P. DUNCAN (1981) Characteristics of the currents east and south of Madagascar. *Deep-Sea Research*, **28**, 879–899.
MCCARTNEY M. (1977) Subantarctic Mode Water. In: *A voyage of discovery: George Deacon 70th anniversary volume*. Supplement to *Deep-Sea Research*, M. ANGEL, editor, Pergamon Press, Oxford, 696 pp.

OLSON D. B. and R. H. EVANS (1986) Rings of the Agulhas Current. *Deep-Sea Research*, **33**, 27–42.
OLSON D. B., R. W. SCHMITT, M. KENNELLY and T. M. JOYCE (1985) A two-layer diagnostic model of the long-term physical evolution of warm-core ring 82b. *Journal of Geophysical Research*, **90**, 8823–8838.
OU H. W. and W. DE RUIJTER (1986) Separation of an inertial boundary current from an irregular coastline. *Journal of Physical Oceanography*, **16**, 280–289.
PATTERSON S. L. (1985) Surface circulation and kinetic energy distributions in the Southern Hemisphere oceans from FGGE drifting bouys. *Journal of Physical Oceanography*, **15**, 865–884.
PEARCE A. F. (1977) Some features of the upper 500 m of the Agulhas Current. *Journal of Marine Research*, **35**, 731–751.
PEARCE A. F. (1980) Early observations and historical notes on the Agulhas Current circulation. *Transactions of the Royal Society of South Africa*, **44**, 205–212.
RICHARDSON P. L. and J. A. KNAUSS (1971) Gulf Stream and western boundary undercurrent observations at Cape Hatteras. *Deep-Sea Research*, **18**, 1089–1110.
ROCHFORD D. J. (1983) Origins of water within warm-core eddies of the western Tasman Sea. *Australian Journal of Marine and Freshwater Research*, **34**, 525–534.
SAETRE R. and A. JORGE DA SILVIA (1984) The circulation of the Mozambique Channel. *Deep-Sea Research*, **31**, 485–508.
SCHMITT R. W. and D. B. OLSON (1985) Wintertime convection in warm-core rings: Thermocline ventilation and the formation of mesoscale lenses. *Journal of Geophysical Research*, **90**, 8823–8838.
SIO DATA REPORT (1985) Physical, Chemical and *In-Situ* CTD Data from the Ajax Expedition in the South Atlantic Ocean, aboard RV *Knorr* Leg I: 7 October–6 November 1983 Leg II: 11 January–19 February 1984. University of California, Scripps Institution of Oceanography and Texas A&M University, Department of Oceanography. S10 Reference 85–24, TAMU Reference 85-4-D.
SPENCER D., W. BROECKER, H. CRAIG and R. WEISS (1982) Geosecs Indian Ocean Expedition, U.S. Government Printing Office, Washington, D.C., Plate 140.
TOOLE J. and M. RAYMER (1985) Heat and fresh water budgets of the Indian Ocean—revisited. *Deep-Sea Research*, **32**, 917–928.
TSUCHIYA M. (1985) Evidence of a double-cell subtropical gyre in the South Atlantic Ocean. *Journal of Marine Research*, **36**, 449–468.
WARREN B. A. (1981a) Transindian hydrographic section at Lat. 18°S: Property distributions and circulation in the South Indian Ocean. *Deep-Sea Research*, **28**, 759–788.
WARREN B. A. (1981b) Note on the shallow oxygen minimum of the South Indian Ocean. *Deep-Sea Research*, **28**, 859–864.
WYRTKI K. (1971) Oceanographic Atlas of the International Indian Ocean Expedition. National Science Foundation, Washington, D.C., 531 pp.
WYRTKI K. (1973) Physical oceanography of the Indian Ocean. In: *Ecological studies. Analysis and synthesis*, Vol. 3, B. ZEITZSCHEL, editor, Springer-Verlag, Berlin, pp. 18–36.